Model-Based Extracted Water Desalination System for Carbon Sequestration

Final Report

Project Period of Performance: September 1, 2015 – February 28, 2017

Report Submission Date: May 28, 2017

SUBMITTED UNDER CONTRACT

DE-FE0026308

DUNS Number: 086188401

SUBMITTED BY:

General Electric Global Research Center

1 Research Circle

Niskayuna, NY 12309

PRINCIPAL INVESTIGATOR

Elizabeth M. Dees, Lead Chemical Engineer

Submitted on behalf of GE by David R. Moore, Technical Operations Leader

Phone: 518-387-5326; Email: moored@research.ge.com

TEAMING PARTNERS - PENNSYLVANIA STATE UNIVERSITY

Prof. Li Li , Associate Professor, Department of Civil & Environmental Engineering

Phone: 814-867-0151; Email: lili@engr.psu.edu

Prof. Manish Kumar, Associate Professor, Department of Chemical Engineering

Phone: 814-865-7519; Email: mxk64@psu.edu

SUBMITTED TO

U.S. Department of Energy

National Energy Technology Laboratory

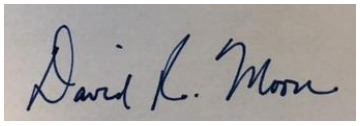

Table of Contents

I. Executive Summary 5
Deep saline formation characterization 5
Technoeconomic analysis of desalination technologies 5
Pre-pilot process validation 6
Scope of Field Pilot 6
II. Research Findings and Accomplishments 6
A. Introduction 6
B. Project Goals 7
C. Major Activities and Results 7
1. Task 2: Identify Extracted Water Source and Establish Partnership with CO_2 Injection Site Operator 7
2. Task 3: Technoeconomic analysis of desalination technologies 14
3. Task 4: Pre-pilot process validation 39
4. Pilot System Conceptual Design 51
D. Future Efforts 52
III. Limitations on Public Release 53
IV. Acknowledgement and Disclaimer 53
V. Appendix: Survey of Deep Saline Formation Mineralogy and Water Chemistry 54
A. Survey of DOE 1260 Sites 54
B. Formation water chemistry 57
C. Map of Formation Water TDS and Lithology 59
VI. Bibliography 61

Table of Figures

Figure 1. Project Overview *6*
Figure 2. Hydraulic Fracturing Water Use Map (Kondash & Vengosh, 2015) *9*
Figure 3. FGD Wastewater and Other Waste Streams (GE Power, Water & Process Technologies, 2016) *11*
Figure 4. Total Desalination Capacity by Country in 2006 (Zander, et al., 2008) *12*

Figure 5. Desalination Capacity in the United States and Worldwide 1950-2006 (International Desalination Association, 2006) 12
Figure 6. NaOH-Na_2CO_3 Softening: Mg^{2+} Precipitation with NaOH 15
Figure 7. NaOH-Na_2CO_3 Softening: Ca^{2+} Precipitation with Na_2CO_3 16
Figure 8. Simplified Block Flow Diagram for Extracted Water Recovery 18
Figure 9. Diagram of Falling Film Mechanical Vapor Recompression Evaporator System 18
Figure 10. Sensitivity of Desalination Cost to Reinjection Cost 21
Figure 11. Water Lifecycle of Base Case: Key Flow Rates and Compositions 21
Figure 12. Schematic of FO Desalination System (McGovern & Lienhard, 2014) 24
Figure 13. Membrane Distillation Schematic (Yarlagadda, Camacho, Gude, & Wei, 2009) 27
Figure 14. Schematic Diagram of Proposed HDH Desalination Process 28
Figure 15. Process Flow Diagram: Desalination via Turbo-expander Technology 29
Figure 16. Design Cases for HPRO vs. FF-MVR Technoeconomic Analysis 31
Figure 17. Base Case 2x SWRO System for Comparison to Hybrid SWRO + HPRO System 35
Figure 18. Hybrid SWRO + HPRO System Cases Studied 35
Figure 19. Cost Breakdown of Hybrid SWRO + HPRO System Cases 37
Figure 20. Base Case FF-MVR + XTL FGD Wastewater Treatment System 38
Figure 21. RO Preconcentration (SWRO or SWRO + HPRO) FGD Wastewater Treatment Cases Studied 38
Figure 22. Single Channel Microclarifier Prototype 41
Figure 23. Microclarifier Performance with Field-sourced Produced Water 41
Figure 24. Prototype Microclarification Unit 42
Figure 25. Prototype Microclarifier Performance with (a) Bakken and (b) Eagle-Ford Production Water. 42
Figure 26. Candle Filter used in 0.5 gpm Tests 43
Figure 27. Performance Comparison: Coated (oil-tolerant) vs. Uncoated Microfiltration Membranes with Synthetic Produced Water 44
Figure 28. Microfiltration Unit in GRC Pre-pilot Facility 45
Figure 29. Microfilter Performance with Bakken Production Water 45
Figure 30. Schematic Diagram of Spiral-wound UF Element 46
Figure 31. Photographs of Sample Vials Before and After M-Series UF Pretreatment 46
Figure 32. Ultrafiltration Unit in GRC Pre-pilot Facility 47
Figure 33. Steam-regenerable Sorption Unit in GRC Pre-pilot Facility: (a) Resin Column and (b) Steam Generator 48
Figure 34. Toluene Breakthrough Curves for Steam Regenerable Sorbent 49
Figure 35. Condensate Recovered During Steam Regeneration 49
Figure 36. Brine Concentrator: Onset of NaCl Crystallization 50
Figure 37. Reverse Osmosis Element Configuration 51
Figure 38. Conceptual Design for Pretreatment 52
Figure 39. GRC Pilot Coating Infrastructure: (a) Phase Inversion Ultrafiltration and (b) Thin Film Interfacial Polymerization Coating Lines. 53
Figure 40. Formation water composition from NatCarb brine database 59
Figure 41. Map of Produced Water TDS 60
Figure 42. Map of Lithology 60

Table of Tables

Table 1. Project Milestones 7
Table 2. Water Use and Production of Major Unconventional Oil & Gas Plays (Kondash & Vengosh, 2015) 9
Table 3. FGD Wastewater Composition (Brooks Rand Labs, 2016) 11
Table 4. Worldwide Desalination and Seawater RO Capacity (Global Water Market, 2017) 13
Table 5. Opportunity for Further Concentration of Seawater RO Concentrate 13
Table 6. Design Case Feed Composition (NR = not reported) 14
Table 7. Softening Chemical and Sludge Disposal Costs 15
Table 8. Material Balance and Costs for Softening Design Case Feed Water 17
Table 9. Costs Included in Base Case Analysis 19
Table 10. Parameters for Desalination Cost Calculations 20
Table 11. Normalized Water Recovery Cost 20
Table 12. Material Balance for Base Case 22
Table 13. FO Design and Operating Parameters 25
Table 14. Forward Osmosis Cost Parameters 26
Table 15. Estimated Forward Osmosis Costs 26
Table 16. MD Desalination Cost Comparison: Direct Heating vs. MVR 27
Table 17. HDH Normalized Cost Estimation 28
Table 18. Estimated Normalized Costs for Turbo-expander-based Freeze Desalination 29
Table 19. Properties of high-pressure RO feed waters 30
Table 20. Normalized Energy Cost of High Pressure Reverse Osmosis 31
Table 21. HPRO Feed Pressure and Concentrate Concentration 32
Table 22. Material Factors for Corrosion-Resistant Alloys 32
Table 23. Normalized Cost of HPRO 34
Table 24. Normalized Cost of High TDS Desalination Technologies 34
Table 25. Normalized Cost of Hybrid SWRO + HPRO System Cases Studied 36
Table 26. HPRO Feed Pressure and Concentrate Concentration 38
Table 27. Normalized Cost of RO Preconcentration (SWRO or SWRO + HPRO) FGD Wastewater Treatment Cases Studied 39
Table 28. Pilot-ready Extracted Water Pretreatment Technologies 40
Table 29. DOE 1260 Phase 1 Site Summary 54
Table 30. Geological Characterization of DOE 1260 Phase 1 Sites 55
Table 31. Mineral Compositions (wt%) 56
Table 32. Formation Water Characterization 57
Table 33. Formation Water Chemistry (units: mg/L) 58

I. Executive Summary

Over the last 1.5 years, GE Global Research and Pennsylvania State University defined a model-based, scalable, and multi-stage extracted water desalination system that yields clean water, concentrated brine, and, optionally, salt. The team explored saline brines that ranged across the expected range for extracted water for carbon sequestration reservoirs (40,000 up to 220,000 ppm total dissolved solids, TDS). In addition, the validated the system performance at pilot scale with field-sourced water using GE's pre-pilot and lab facilities.

This project encompassed four principal tasks, in addition to Project Management and Planning: 1) identify a deep saline formation carbon sequestration site and a partner that are suitable for supplying extracted water; 2) conduct a techno-economic assessment and down-selection of pre-treatment and desalination technologies to identify a cost-effective system for extracted water recovery; 3) validate the downselected processes at the lab/pre-pilot scale; and 4) define the scope of the pilot desalination project. Highlights from each task are described below:

Deep saline formation characterization

The deep saline formations associated with the five DOE NETL 1260 Phase 1 projects were characterized with respect to their mineralogy and formation water composition. Sources of high TDS feed water other than extracted water were explored for high TDS desalination applications, including unconventional oil and gas and seawater reverse osmosis concentrate.

Technoeconomic analysis of desalination technologies

Techno-economic evaluations of alternate brine concentration technologies, including humidification-dehumidification (HDH), membrane distillation (MD), forward osmosis (FO), turboexpander-freeze, solvent extraction and high pressure reverse osmosis (HPRO), were conducted. These technologies were evaluated against conventional falling film-mechanical vapor recompression (FF-MVR) as a baseline desalination process. Furthermore, a quality function deployment (QFD) method was used to compare alternate high TDS desalination technologies to FF-MVR. High pressure reverse osmosis was found to a be a promising alternative desalination technology. A deep-dive technoeconomic analysis of HPRO was performed, including Capex and Opex estimates, for seawater RO (SWRO). Additionally, two additional cases were explored: 1) a comparison of a SWRO plus HPRO system to the option of doubling the size of a standard seawater RO system to achieve the same total pure water recovery rate; and 2) a flue gas desulfurization wastewater treatment zero-liquid discharge (ZLD) application, where preconcentration with RO (SWRO or SWRO + HPRO) before evaporation and crystallization was compared to FF-MVR and crystallization technologies without RO preconcentration.

Pre-pilot process validation

Pre-pilot-scale tests were conducted using field production water to validate key process steps for extracted water pretreatment. Approximately 5,000 gallons of field produced water was processed through, microfiltration, ultrafiltration, and steam regenerable sorbent operations. Smaller quantities were processed through microclarification. In addition, analytical methods (purge-and-trap gas chromatography and Hach TOC analytical methods) were validated. Lab-scale HPRO elements were constructed and tested at high pressures, to identify and mitigate technical risks of the technology. Lastly, improvements in RO membrane materials were identified as the necessary next step to achieve further improvement in element performance at high pressure.

Scope of Field Pilot

A field pilot for extracted water pretreatment was designed.

II. Research Findings and Accomplishments

A. Introduction

This final report summarizes activities throughout the program period. The overall project scope is summarized in Figure 1.

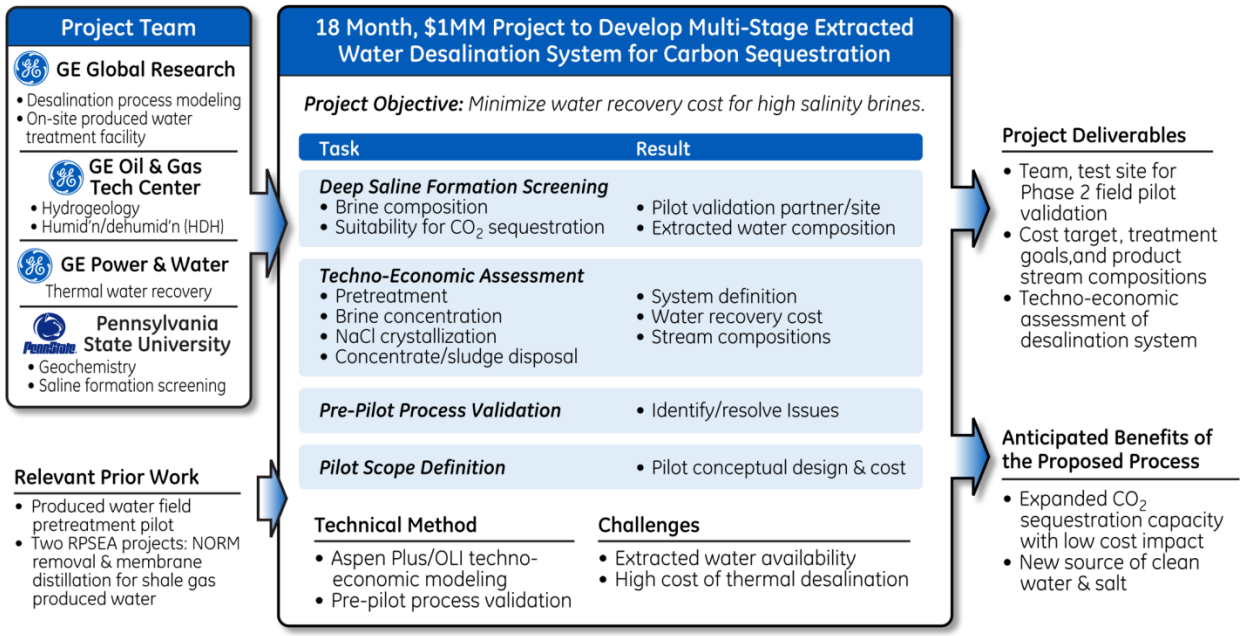

Figure 1. Project Overview

B. Project Goals

The key goals of this project are:

1. Define the scope and identify a team and test location for pilot-scale implementation of the desalination system.
2. Define a scalable, multi-stage extracted water desalination system that yields clean water, concentrated brine, and, optionally, salt from saline brines (180,000 ppm total dissolved solids, TDS) and that meets a cost target.
3. Validate the overall system performance with field-sourced water using GE pre-pilot and lab facilities.

The milestones stated in the proposal are listed in Table 1.

Table 1. Project Milestones

Milestone Title	Planned Completion Date	Actual Completion Date	Comments
Carbon sequestration site and partner identified for extracted water recovery pilot validation	3/31/2016	12/31/2015	Identified two Phase 1 1260 award winners as partners with whom to submit Phase 2 applications
Cost-effective extracted water desalination system for site identified in Task 2 defined	6/30/2016	3/31/2016	Completed pretreatment system design and desalination technology ranking
Project final report completed	2/28/2017	5/28/2017	Results summarized and submitted

C. Major Activities and Results

1. <u>Task 2: Identify Extracted Water Source and Establish Partnership with CO_2 Injection Site Operator</u>

During the proposal phase of this project, the team understood that it was necessary to identify a partner from among all the Carbon Capture and Sequestration (CCS) sites and operators in the United States to obtain extracted water and to pursue definition of Phase 2 of the Brine Extraction and Storage Test (BEST) project. GEGR partnered with The Pennsylvania State University (PSU) to investigate the suitability of each of the BEST Phase 1 sites for a BEST Phase 2 field project, particularly with respect to formation water composition and geochemistry. Dr. Li Li, associate professor of Department of Civil & Environmental

Engineering, and her team, reviewed publicly available information on each potential Phase 2 field site with respect to water composition.

After this project was awarded, it became clear that the BEST site(s) would be chosen from among the five Phase 1 award winners, which made the task of selecting a potential partner significantly simpler. Therefore, this task was reshaped to focus on screening and characterizing deep saline formations to define the range of extracted water compositions and help define appropriate water pretreatment and desalination technologies. The details of this activity are included in the appendix. The appendix includes a survey of the mineralogy and formation water composition for the DOE 1260 sites, and an initial overview of deep saline formation water compositions in the continental United States.

While the initial focus of this project was water recovery from high-TDS extracted waters (~180,000 mg/L), sites with *low*-TDS extracted waters (e.g., University of Texas, Austin) were still of interest because a vast majority of CCS sites contain water with low TDS. A combination of water recovery technologies could be employed at such sites. Thus, high pressure reverse osmosis, electrodialysis reversal (EDR), or a simple boiler may be used to partially desalinate pretreated low-TDS extracted water to generate a high-TDS intermediate product (e.g., 150,000-180,000 mg/L TDS). It was envisioned that this intermediate product could then be tested by one or more high-TDS desalination process of interest.

Sources of high TDS feed water other than extracted water were explored for high TDS desalination applications. Since there are a limited number of extracted water sources and the sites for the 1260 Phase 2 pilots were already selected, understanding of other types of waters that could benefit from high TDS desalination technologies will broaden the opportunity for these technologies. Unconventional oil and gas, coal-fired power and seawater reverse osmosis concentrate are three application spaces that were explored.

a. <u>Unconventional oil and gas</u>

Large volumes of water are withdrawn from ground water and/or surface water to be used in the hydraulic fracturing process, which has a significant impact on water availability, particularly in already water stressed regions. A recent report found that nearly half (47%) of oil and gas wells recently hydraulically fractured in the U.S. are in regions with high or extremely high water stress (Freyman, February 2014). The shale plays where hydraulic fracturing dominated the majority of oil and gas drilling have water use ranging between 0.39 million gallons and 6.27 million gallons of water per well, with the Woodford, Marcellus, Haynesville, and Fayetteville plays having some of the highest water usage per well, as shown in Figure 2 (Kondash & Vengosh, 2015).

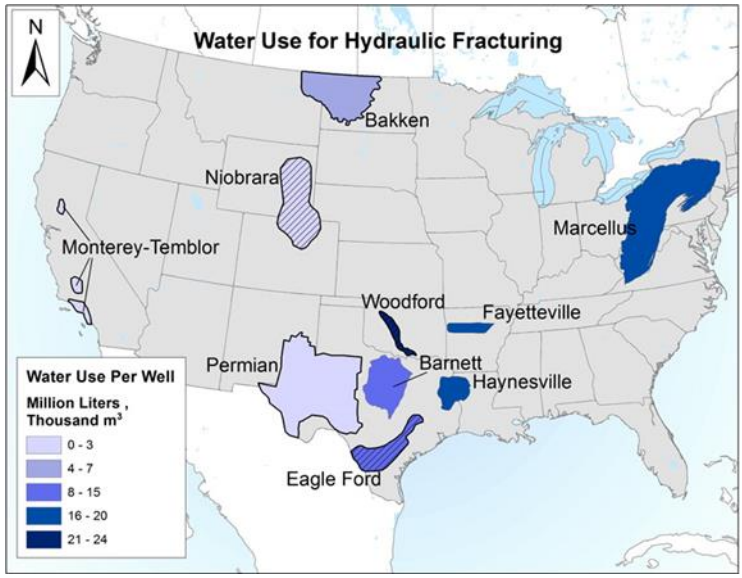

Figure 2. Hydraulic Fracturing Water Use Map (Kondash & Vengosh, 2015)

Following hydraulic fracturing, flowback water made up mostly of injected hydraulic fracturing fluids (with some formation water) is the first water produced from a well. Over time the composition of the water produced along with the oil or gas becomes almost entirely formation water. Fractured wells typically have high wastewater production rates in the first two to three years, then produced water rates gradually decrease parallel to the oil or gas production (Kondash & Vengosh, 2015). Table 2 summarizes water use and wastewater production per well for the major unconventional oil and gas plays.

Table 2. Water Use and Production of Major Unconventional Oil & Gas Plays (Kondash & Vengosh, 2015)

Shale gas	Water use (10^6 gal/well)	Flowback & produced water (10^6 gal/well)	Unconventional oil	Water use (10^6 gal/well)	Flowback & produced water (10^6 gal/well)
Barnett	3.80	3.28	Bakken	1.97	3.24
Eagle Ford	3.61	6.83	Permian	0.80	
Fayetteville	5.29		Monterey-Temblor	0.07	3.78
Haynesville	5.13	4.63	Eagle Ford	3.97	6.01
Marcellus	4.25	1.37	Niobrara	0.34	0.34
Niobrara	0.39	1.50	Woodford	2.05	2.05
Woodford	6.27				

Hydraulic fracturing is a water-dependent and water-intense production activity. The high demand for water and stringent environmental regulations make wastewater management an

essential part of the oil and gas business. Produced water treatment practices vary widely, and are driven by local environmental regulations and disposal costs. In locations where produced water treatment is desirable (e.g., due to the high cost of hauling wastewater from areas where deep-well injection is prohibited), water treatment solutions, including desalination, are needed. While the produced water from some locations, such as the Marcellus and Bakken, is typically near or beyond saturation (~240,000-310,000 mg/L TDS) (U.S. Geological Survey National Produced Waters Geochemical Database, 2016), others, including the Barnett and Permian Basin, have much lower TDS levels (~20,000-100,000 mg/L for the Barnett (Hayes, 2011) and ~20,000-45,000 mg/L for the Permian Basin (Technical Bulletin: Water Quality Variability During Oilfield Wastewater Treatment for Frac Reuse, 2016)). Thus, desalination technologies applicable to a wide range of water compositions, from seawater salinity to saturation, are needed to treat produced water from hydraulic fracturing.

b. Coal-fired power

Coal is plentiful and affordable, and accounts for about 37% of all electricity generated in the United States (U.S. Energy Information Administration, 2016). Coal-fired power plants are required by the US EPA to remove sulfur dioxide emissions from the flue gas they generate. Over 85% of flue gas desulfurization (FGD) systems employ wet scrubbers that use a slurry of alkaline sorbent, usually limestone ($CaCO_3$) or lime (CaO), to scrub gases and convert gaseous sulfur dioxide to calcium sulfate particulates. In addition to FGD wastewater, fly ash leachate (fly ash is the non-combustible portion of coal) is the other main wastewater from coal-fired power operations. FGD wastewater and other wastewater streams generated by coal-fired power plants are depicted in Figure 3. The FGD wastewater composition given in Table 3 indicates TDS levels are typically < 70,000 mg/L.

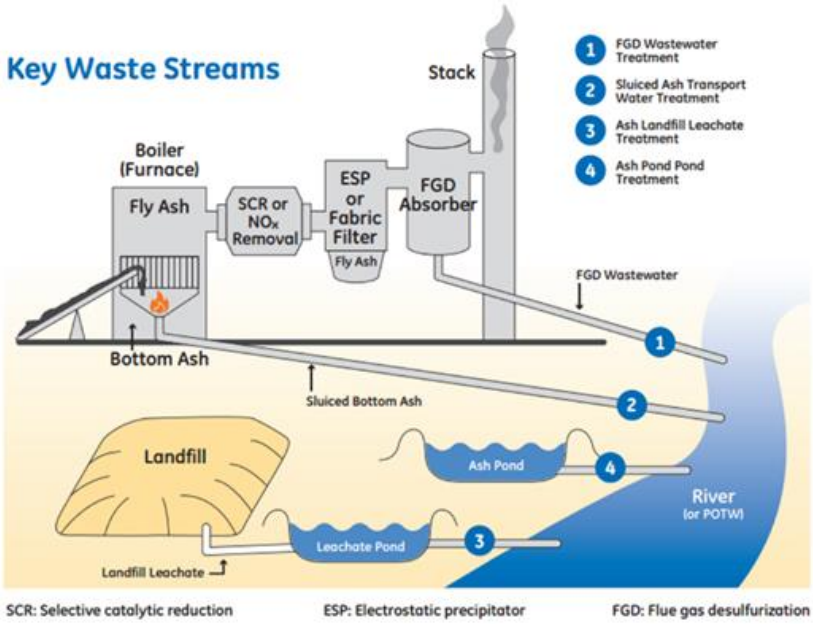

Figure 3. FGD Wastewater and Other Waste Streams (GE Power, Water & Process Technologies, 2016)

Table 3. FGD Wastewater Composition (Brooks Rand Labs, 2016)

Chemical	Amount (mg/L)
pH	4.5 – 9.0
Total suspended solids	< 10 – 170,000
Total dissolved solids	4,000 – 68,000
Total organic carbon	5 – 1,100
Sulfate	4,500 – 22,000
Chloride	1,000 – 28,000
Calcium	600 – 5,700
Magnesium	400 – 7,700
Sodium	20 – 4,800

c. Seawater reverse osmosis concentrate

The number of people worldwide who experience water scarcity is expected to grow from 700 million today to 1.8 billion by 2025. Many countries around the world, including Israel, Singapore, and Japan, currently rely heavily on desalination technologies to meet fresh water demands. Other countries, including the United States, are expected to expand desalination capacity in the future to address growing water scarcity issues. Figure 4 shows the total desalination capacity by country in 2006 (Zander, et al., 2008). As shown in Figure 5, total worldwide online desalination capacity was approximately 37.8 million m^3/day (10 billion gallons/day) in 2006, up from approximately 5 million m^3/day (1.3 billion gallons/day) in 1980. In 2006, US online capacity was approximately 5 million m^3/day (International Desalination Association, 2006).

Desalination capacity indicates the desalinated water production rate, and since typical seawater reverse osmosis desalination plants recover 50% of the feed water, an equal amount of concentrated brine is produced (i.e., 1:1 desalinated water:concentrated brine production rate). Although desalination capacity includes both brackish water and seawater desalination, using the 1:1 desalinated water:concentrated brine ratio for seawater desalination leads to an estimated worldwide concentrated brine production rate of 37.8 million m^3/day (10 billion

gallons/day) in 2006. Further treatment of this concentrated brine, typically ~70,000 mg/L TDS, represents a vast opportunity for high TDS desalination technology to increase fresh water production from standard seawater reverse osmosis desalination plants.

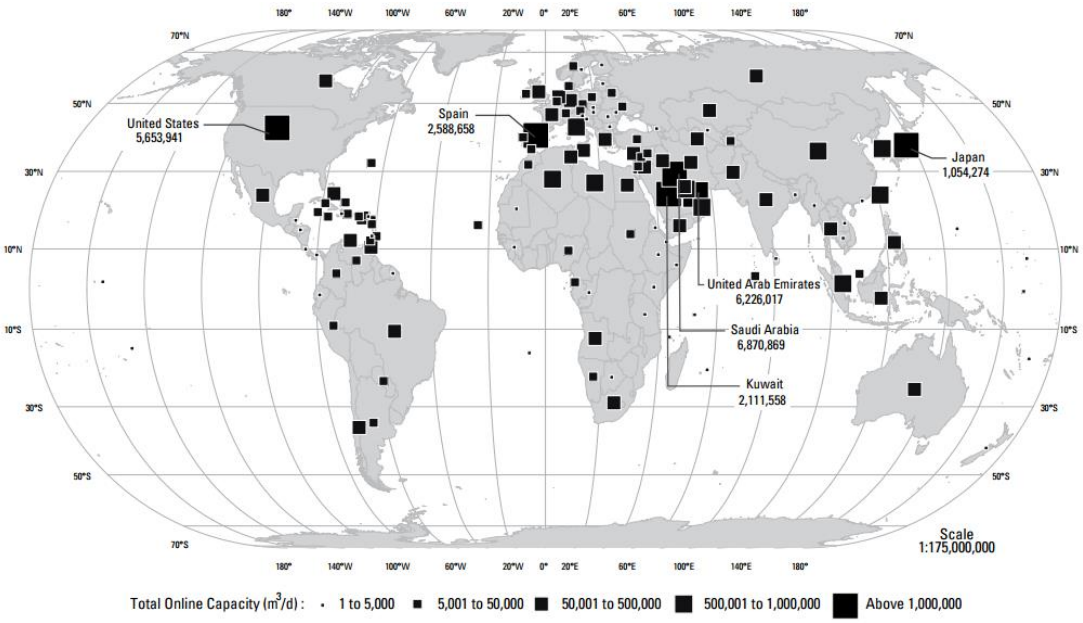

Figure 4. Total Desalination Capacity by Country in 2006 (Zander, et al., 2008)

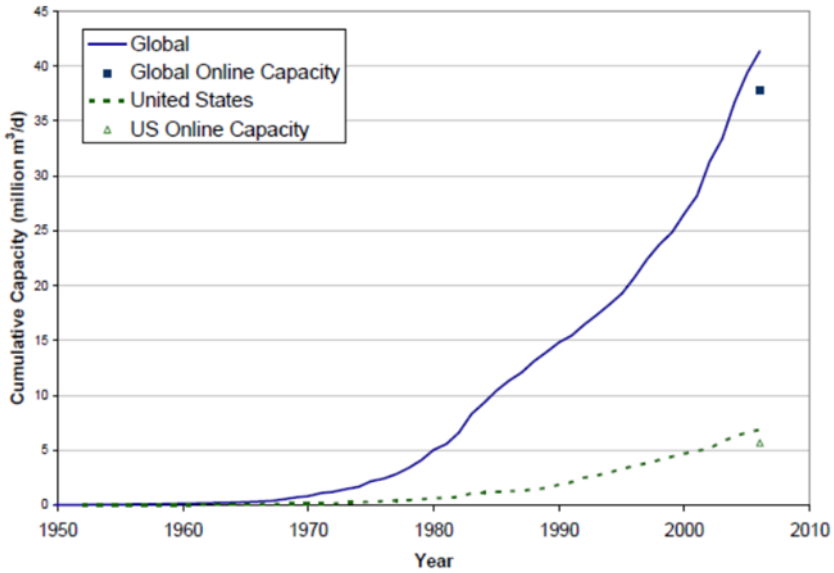

Figure 5. Desalination Capacity in the United States and Worldwide 1950-2006 (International Desalination Association, 2006)

Typical seawater reverse osmosis (SWRO) desalination plants operate at 50% (or lower) recovery, which means they leave at least 50% of the incoming water unusable. Higher recovery is desirable for many reasons, including increasing demands for desalinated water and more

stringent (and costly) requirements for brine discharge. Table 4 includes GWI data and projections for worldwide desalination capacity and fractional capacity accounted for by membrane (vs. thermal) technology and seawater (vs. brackish water) feed (Global Water Market, 2017). These data were used to calculate a total projected 2020 SWRO capacity of 14.3 BB GPD. Assuming 50% recovery of SWRO, desalinated water production (i.e., SWRO capacity) and SWRO concentrate production may be approximated as equal. Therefore, by 2020, it is projected that 14.3 BB GPD of SWRO concentrate will be produced.

Table 4. Worldwide Desalination and Seawater RO Capacity (Global Water Market, 2017)

	Desalination (BB GPD)	Fraction membrane	Fraction seawater	Seawater RO (BB GPD)
1990 capacity	4	0.5*	0.5*	1
1990-2014 additional capacity	20	0.75	0.68	10
2015-2020 projected additional capacity	4.8	0.91	0.76	3.3
Total 2020 projected capacity	28.8	-	-	14.3

*Not reported in (Global Water Market, 2017), so conservative estimates were used.

Using an average seawater TDS of 35,000 mg/L and the assumption of 50% SWRO recovery, SWRO concentrate TDS will be approximately 70,000 mg/L. The opportunity associated with further concentration of this SWRO concentrate was estimated for the five final concentrate TDS levels and corresponding additional water recoveries shown in Table 5. As can be seen from Table 5, concentrating the available SWRO concentrate to 100,000 mg/L TDS would provide an additional 4.3 BB GPD of desalinated water, and reduce the amount of concentrate that must be disposed of from 14.3 to 10.0 BB GPD. If the available SWRO concentrate was concentrated to saturation (i.e., 295,000 mg/L TDS), an additional 11.0 BB GPD of desalinated water would be produced and the amount of concentrate requiring disposal would be decreased from 14.3 to 3.3 BB GPD.

Table 5. Opportunity for Further Concentration of Seawater RO Concentrate

Final concentrate TDS (mg/L)	100,000	130,000	175,000	245,000	295,000
Additional recovery (%)	30	46	60	72	77
Additional product water (BB GPD)	4.3	6.6	8.6	10.3	11.0
Concentrate remaining (BB GPD)	10.0	7.7	5.7	4.0	3.3

2. Task 3: Technoeconomic analysis of desalination technologies

a. Identification of promising pretreatment technologies

Pretreatment: Softening

Field water samples received from UT Austin (Eagle-Ford shale oil produced water) and from EERC (Bakken shale oil produced water) were found to have high hardness levels. Some desalination technologies (e.g., reverse osmosis, electrodialysis, humidification-dehumidification) are sensitive to hardness, and softening would therefore be a required part of the pretreatment process if one of these technologies is to be implemented for treatment of high hardness extracted waters. A design case feed composition based on the average of four Bakken production water samples, diluted with water to 180 g/L TDS, was used in an Aspen Plus™ model to calculate the quantity of softening chemicals required and the amount of sludge generated in softening the feed. The design case feed composition is given in Table 6 below.

Table 6. Design Case Feed Composition (NR = not reported)

Analyte	mg/L
B	NR
Li	NR
Na	48,782
K	5079
Mg	710
Ca	14,884
Sr	1273
Ba	NR
Fe	NR
Mn	NR
P	<15
Si	<20
Fluoride	<7
Sulfate	14
NO_2 & NO_3 (as Nitrogen)	<4
Bromide	100
Chloride	109,258
TSS	500
TOC	170
TDS	180,000
Total Hardness as $CaCO_3$	40,089

The chemical softening process uses NaOH to precipitate Mg^{2+} and Na_2CO_3 to precipitate Ca^{2+} and Sr^{2+}, as shown in the following equations:

$$MgCl_2 + 2NaOH \rightarrow Mg(OH)_{2(s)} + 2NaCl$$
$$CaCl_2 + Na_2CO_3 \rightarrow CaCO_{3(s)} + 2NaCl$$
$$SrCl_2 + Na_2CO_3 \rightarrow SrCO_{3(s)} + 2NaCl$$

Figure 6 shows the effect of NaOH addition on the residual Mg^{2+} in solution. Approximately 2.1 mole NaOH per mole Mg^{2+} is required to fully precipitate the magnesium. Figure 7 shows the effect of Na_2CO_3 addition on residual Ca^{2+} in solution. Approximately 1.1 mole Na_2CO_3 per mole Ca^{2+} is needed to fully precipitate the calcium.

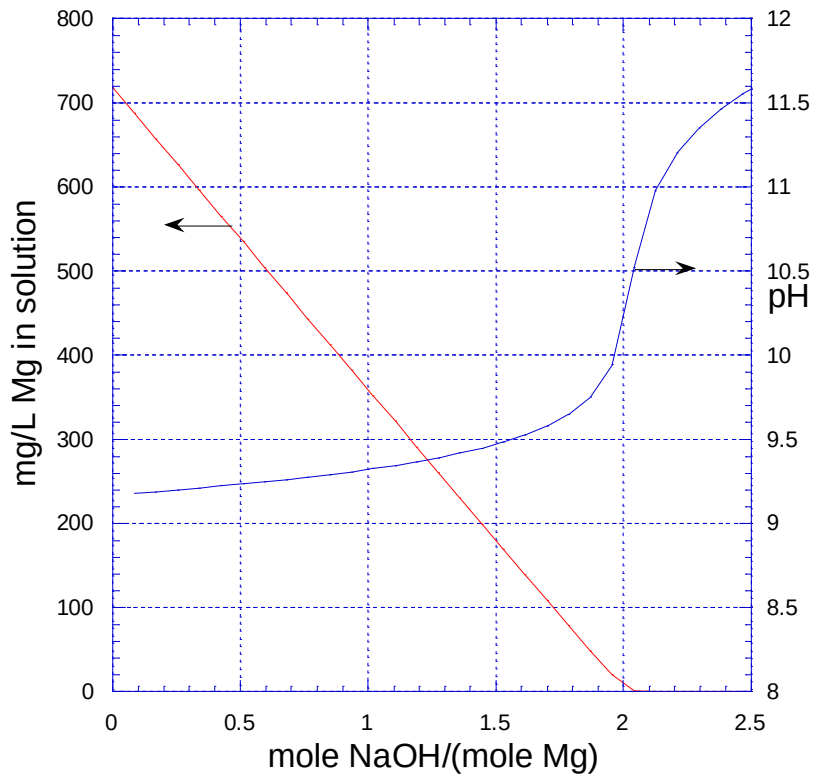

Figure 6. NaOH-Na_2CO_3 Softening: Mg^{2+} Precipitation with NaOH

Table 7. Softening Chemical and Sludge Disposal Costs

	Units	Cost
HCl as 32% solution	$/lb as 100%	$0.238
NaOH as 50% solution	$/lb as 100%	$0.277
Na_2CO_3 dry solid	$/lb as 100%	$0.159
Sludge disposal cost	$/short ton	$50

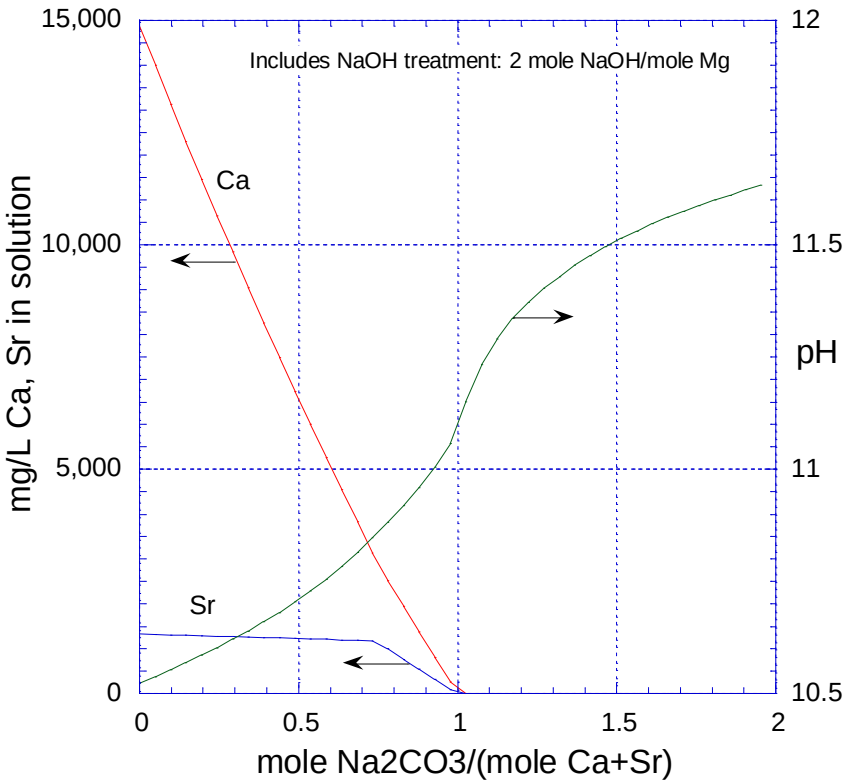

Figure 7. NaOH-Na_2CO_3 Softening: Ca^{2+} Precipitation with Na_2CO_3

The cost of softening was calculated using sufficient NaOH and Na_2CO_3 to precipitate essentially all the Group 2 cations, followed by addition of HCl to neutralize the softened brine to about pH 6.5. Table 7 shows the costs for both softening chemicals and sludge disposal. It is assumed that all softening sludge may be disposed of as nonhazardous waste in a RCRA-D landfill. Table 8 shows the softening material balances and costs for both pilot and commercial-scale plants, where the gross distillate rate includes a portion of the water introduced with the softening chemicals.

As is clear from Table 8, the cost for softening chemicals and sludge disposal is prohibitive for the design case feed composition. Thus, the most favorable desalination technologies for this particular environment are those that do not require softening. The Phase 2 BEST pilot test bed may still be an appropriate venue for testing technologies that require softening, e.g., electrodialysis, because there are many saline formations that have considerably lower hardness than the design case brine and may thus be able to be economically softened.

Table 8. Material Balance and Costs for Softening Design Case Feed Water

	Units	Pilot Scale	Commercial Scale
Feed Rate	gpm	10	500
Feed Mg^{2+}	lb-mole/hr	0.147	7.35
Feed Ca^{2+}	lb-mole/hr	1.856	92.81
NaOH needed (100%)	lb/hr	11.50	575.0
Na_2CO_3 needed (100%)	lb/hr	210.1	10,504.3
HCl needed (100%)	lb/hr	1.44	72.0
Sludge generated (25 wt% solids)	short ton/hr	0.411	20.54
NaOH cost	$/hr	$3.18	$159.1
Na_2CO_3 cost	$/hr	$33.51	$1675
HCl cost	$/hr	$0.343	$17.14
Sludge disposal	$/hr	$20.54	$1027
Total softening cost	$/hr	$57.57	$2,878
Gross distillate	m^3/hr	1.123	56.17
Net distillate	m^3/hr	0.8916	44.58
Softening cost	$/$m^3$ gross distillate	$51.25	$51.25
Softening cost	$/$m^3$ net distillate	$64.6	$64.6

b. Identification of promising desalination technologies

Base Case Desalination Technology Definition

Three options were considered in defining the base case technology for high-TDS brine desalination. Figure 8 shows a simplified block flow diagram of the overall process, which shows the key steps in pretreatment and three major desalination options. Option 1 utilizes a falling film thermal brine concentrator with mechanical vapor recompression (FF-MVR). Option 2A utilizes a forced-circulation crystallizer with mechanical vapor recompression (FCC-MVR). Option 2B utilizes a FF-MVR followed by a FCC-MVR.

GE's Water & Process Technology's Thermal Products Division is the leading supplier of large-scale FF-MVR and FCC-MVR systems. Although these thermal brine concentrators and crystallizers are capital-intensive, they have a proven record of reliability, with the vast majority of all units originally installed still in service. As of 2008, of approximately 90 zero liquid discharge (ZLD) facilities in the United States, 69 are GE systems (Mickley, 2008). Figure 9 shows a schematic drawing of a GE thermal brine concentrator.

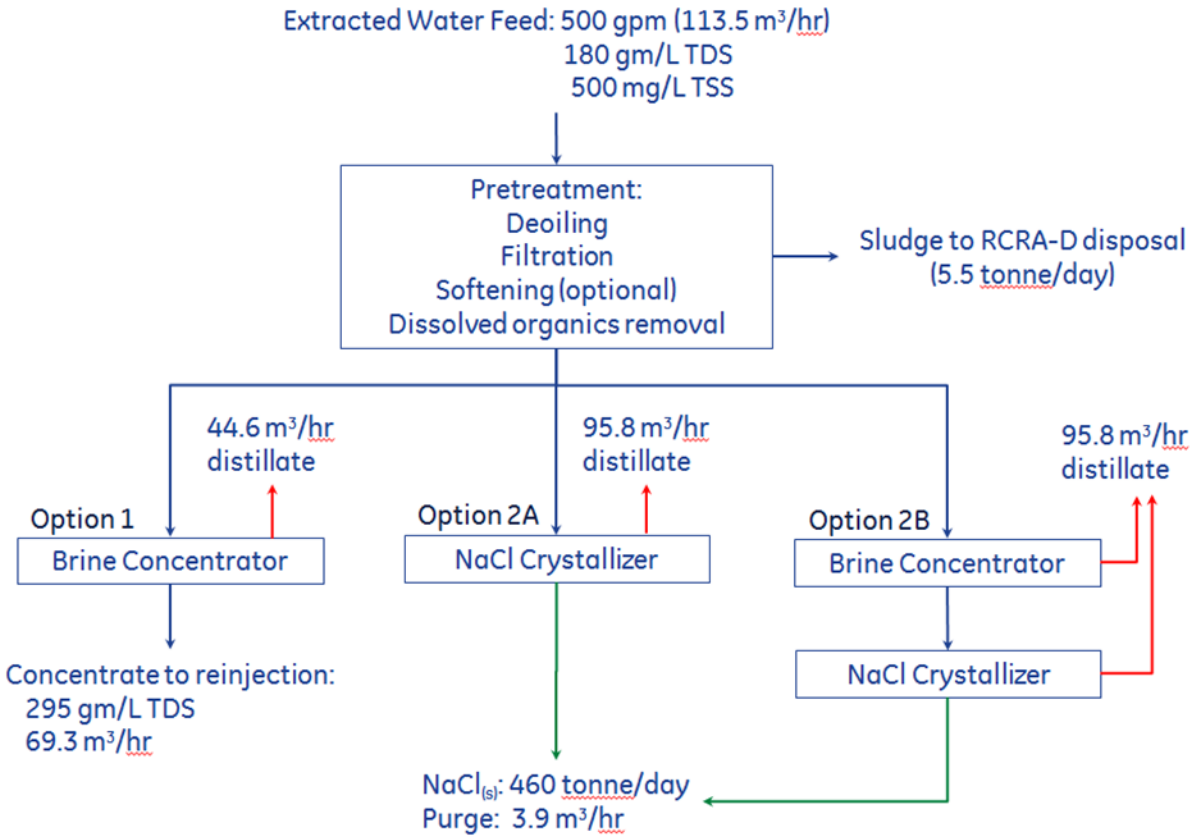

Figure 8. Simplified Block Flow Diagram for Extracted Water Recovery

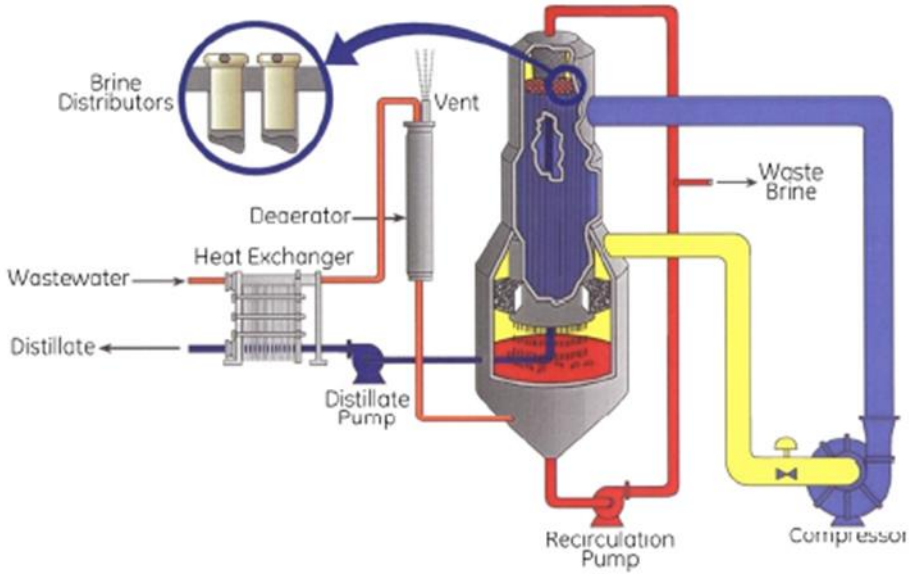

Figure 9. Diagram of Falling Film Mechanical Vapor Recompression Evaporator System (Heins, 2006)

The desalination cost basis is taken to be the cost of recovering a cubic meter of clean water from raw high-TDS (180 gm/L) extracted water containing 500 mg/L of suspended solids. This basis was chosen because the overall goal of extracted water desalination is the net removal of liquid from deep saline aquifers to accommodate supercritical CO_2 ($scCO_2$). Table 9 lists the costs included in the base case cost analysis.

Because the design case produced water comprises essentially all chloride salts, and because the solubility of chloride salts associated with Group 2 metals (e.g., $MgCl_2$ and $CaCl_2$) exceeds the solubility of NaCl, there is no apparent need *based on scaling* to soften the extracted water prior to thermal desalination. The Group 2 metal chlorides will leave the system in solution, either in the brine concentrate stream leaving the concentrator (Option 1) or in the crystallizer purge (Options 2A and 2B).

For Option 1, the volume of brine concentrate is significant and the cost of brine concentrate disposal must be included in the base case cost comparison. For options 2A and 2B, the purge disposal volume is quite low, but is included in the cost comparison. In North America, the cost for brine disposal by deep well injection (UIC) varies widely, with prices reported in the range of $0.50/bbl (Texas) to $3.80/bbl (Wyoming). It is assumed that commercial carbon capture and storage (CCS) systems will be located close enough to reinjection wells that the concentrate can be transported to the injection well by piping. Therefore, the cost to transport concentrate for reinjection is assumed to be negligible. For this analysis, the cost of reinjection is assumed to be $0.40/bbl.

For Options 2A and 2B, with NaCl crystallization, neither cost nor credit is associated with the solid NaCl product generated. It is expected that additional costs for salt washing, drying, storage, and shipment will substantially offset the revenue from salt sales. The potential volume of solid NaCl from high-TDS extracted water desalination is enormous. For the 500 gpm feed rate under consideration, the estimated solid salt production rate for Options 2A and 2B is approximately 167,000 metric tons/year, which represents 0.6% of the total North American NaCl production in 2008 and is comparable to some commercial salt mining operations, which range from about 100,000-2,500,000 metric tons/year (Schlag, Glauser, & Yokose, 2008).

Table 9. Costs Included in Base Case Analysis

Category	Cost Item
CAPEX	Installed cost of desalination process equipment (FF-MVR and/or FCC-MVR)
OPEX	Electricity cost for vapor compression (FF-MVR and/or FCC-MVR)
OPEX	Cost of reinjection of brine concentrate or crystallizer purge
OPEX	Pretreatment and pretreatment sludge disposal cost

Table 10 shows some key parameters used in calculating the cost to desalinate high-TDS extracted water.

Table 10. Parameters for Desalination Cost Calculations

	Units	Value
Electricity Cost	$/KWH	$0.10
Cost of capital	% of installed CAPEX/year	10
Cost of reinjection	$/bbl	$0.40
Mass fraction solids in raw brine filtration sludge	-	0.25

Table 11 shows the cost estimates for three thermal desalination options. As noted above, the cost of Option 1 is sensitive to the cost of reinjection. Table 11 shows the normalized desalination cost as a function of the cost of reinjection.

Table 11. Normalized Water Recovery Cost

(feed: 113.5 m^3/hr, 180 gm/L extracted water, $0.40/bbl reinjection cost)

	Units	Option 1: FF Evaporator Only	Option 2A: Crystallizer Only	Option 2B: FF Evaporator + Crystallizer
Distillate rate	m^3/hr	44.6	95.8	95.8
Concentrate or purge rate	m^3/hr	69.3	3.9	3.9
Desal CAPEX + electricity[a]	-	1	2.1	1.9
Desal Concentrate disposal[a]	-	1	0.026	0.026
Pretreatment[a]	-	1	0.49	0.49
Normalized cost of water recovery[a]	-	1	1.1	1

[a] All costs reported are normalized to corresponding cost for Option 1

For a concentrate disposal cost of $0.40/bbl or less, which should be achievable for Active Reservoir Management (ARM) operations, Option 1 (FF-MVR brine concentrator) is the lowest cost option. Therefore, FF-MVR brine concentrator technology was selected as the base case for comparison with alternate pilot-ready desalination technologies.

If offtakes for concentrated brine can be identified, such as feed to a chlor-alkali plant, a major cost component of Option 1 would be eliminated, which would make Option 1 even more favorable. Option 1 could also be viewed as the first phase of a more comprehensive facility. If a local market for solid NaCl materializes, a crystallizer and salt handling facility may be added to take advantage of that market.

Based on this analysis, Option 1 is taken to be the base case. Figure 11 shows a summary of the key flow rates and compositions for the base case.

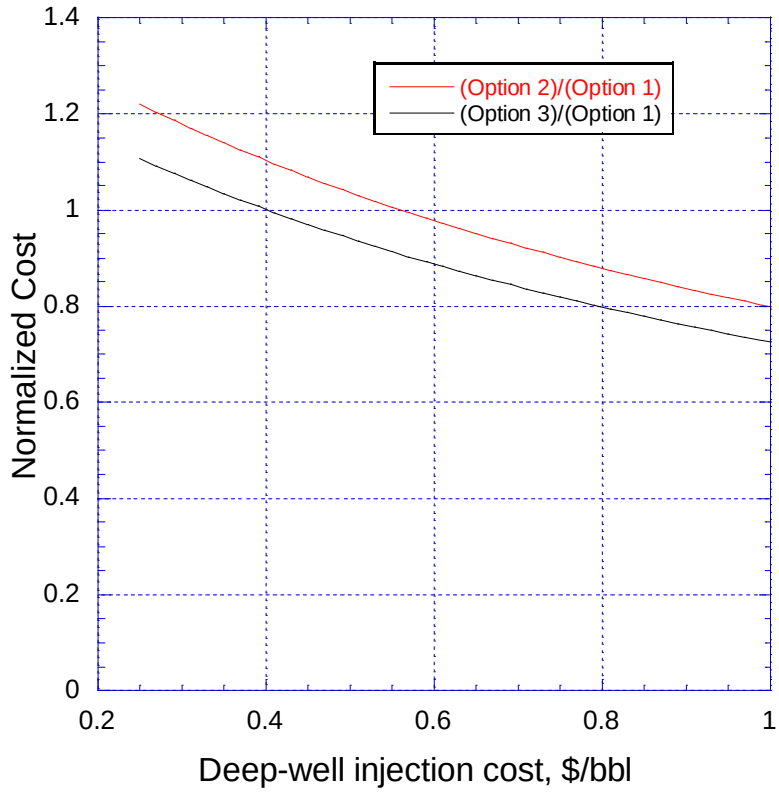

Figure 10. Sensitivity of Desalination Cost to Reinjection Cost

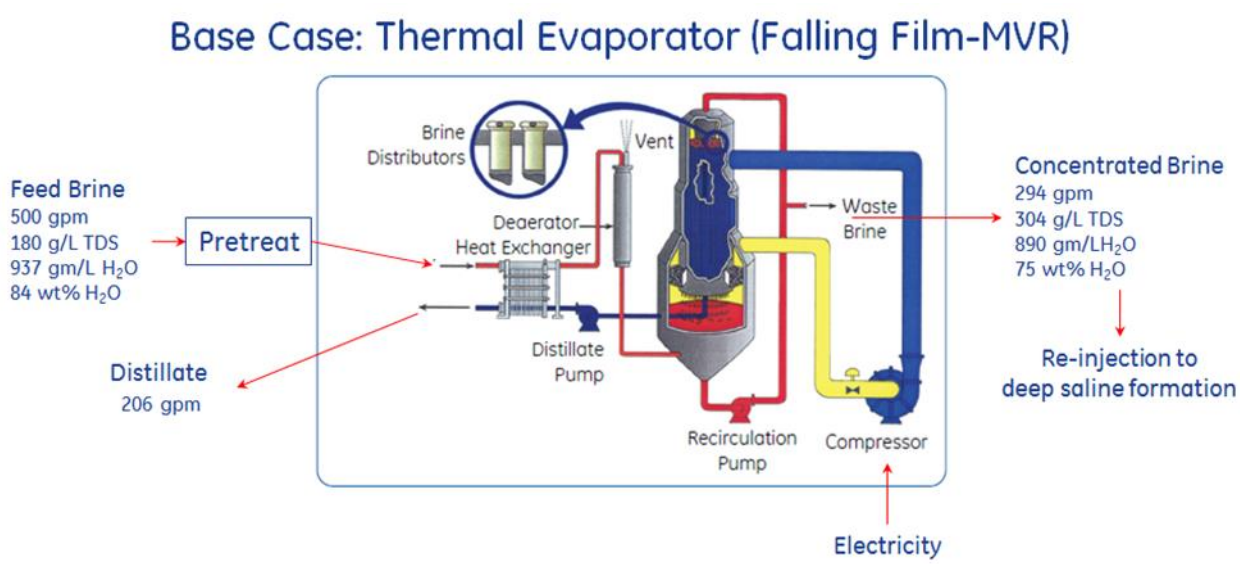

Figure 11. Water Lifecycle of Base Case: Key Flow Rates and Compositions

The material and energy balances for desalination were calculated for design case feed brine that was pretreated for suspended solids and organics removal, but was not softened. Table 12 shows the material balance for the base case desalination process, which is a FF-MVR

brine concentrator that concentrates TSS- and organics-free extracted water (no softening or NaCl crystallization is included). The feed brine is concentrated from 180 gm/L TDS to 295 gm/L TDS and the water recovery on a solids-free basis is 42%.

Table 12. Material Balance for Base Case

Parameter	units	Feed to system	Preheated feed to evaporator	Concentrate to disposal	Distillate
H_2O	lb-mole/hr	12983.38	12944.43	7581.087	5363.342
$CaCl^+$	lb-mole/hr	0.0002744	0.630665	0.010318	0
Ca^{+2}	lb-mole/hr	91.78771	90.88168	91.50228	0
Cl^-	lb-mole/hr	771.7004	768.7549	769.3752	0
H^+	lb-mole/hr	4.79E-05	7.92E-04	1.06E-05	0
Mg^{+2}	lb-mole/hr	7.268042	7.245836	7.246175	0
Na^+	lb-mole/hr	566.1071	564.4088	564.4088	0
Sr^{+2}	lb-mole/hr	3.740711	3.729483	3.729489	0
Total Flow	lb-mole/hr	14423.98	14380.08	9017.36	5363.342
Total Flow lb/hr	lb/hr	278457	277622	180999	96622.44
Total Flow cuft/hr	cu ft/hr	3966.632	4152.384	2414.419	2660280
Temperature	Deg F	68	218.6449	68	225.0056
Pressure	psia	14.69595	14.69595	14.69595	14.69595
Vapor Frac	-	0	0	0	1
Liquid Frac	-	1	1	1	0
Solid Frac	-	0	0	0	0
Enthalpy	BTU/lb-mole	-120320	-117980	-118620	-102870
Enthalpy	BTU/lb	-6232.567	-6110.971	-5909.84	-5710.04
Enthalpy	BTU/hr	-1.74E+09	-1.7E+09	-1.1E+09	-5.5E+08
Entropy	BTU/lb-mole-F	15.48799	18.7473	14.72564	47.04814
Entropy	BTU/lb-F	0.8022732	0.971062	0.73363	2.61156
Density	lb-mole/cu ft	3.63633	3.463091	3.734794	0.002016
Density	lb/cu ft	70.19985	66.85837	74.96592	0.03632
Average MW	lb/lb-mole	19.30514	19.30598	20.0723	18.01534
Liq Vol 60F	cuft/hr	3.88E+03	3.87E+03	2315.03	1550.72
* LIQUID PHASE *					
pH	-	6.534	5.450412	6.662	
TDS (20°C)	mg/L	180109	171537	295006	

Alternate Desalination Technologies

Five alternate brine concentration technologies were compared to the base case technology. The basis of comparison was the cost of desalination for a given technology (CAPEX +OPEX) relative to the cost of the base case technology. The CAPEX is the installed cost for a desalination facility capable of handling 500 gpm feed. OPEX includes energy and consumables (e.g., chemicals, membranes), but does not include labor, maintenance, taxes, or

insurance, as these are expected to be comparable among desalination processes. This analysis provides a methodology for desalination technology selection in Phase 2.

The candidate brine concentration technologies are forward osmosis (FO), membrane distillation (MD), humidification-dehumidification (HDH), clathrates, and turbo-expander freeze desalination (TEF), which is currently supported under DE-FOA-0001095, and high pressure reverse osmosis (HPRO). For this analysis, it is assumed that each alternate technology is capable of generating a 295 gm/L concentrate. Thus, the fraction water recovery is the same for all brine concentration technologies. The differences are in the capital and operating costs. The equipment sizing and normalized cost calculations are reported in this section. All costs are normalized by the corresponding cost for the FF-MVR base case. For example, the normalized energy cost is the energy cost for a given technology divided by the energy cost for the base case. All costs are in terms of $\$/m^3$ product water.

Desalination technologies developed under DE-FOA-0001238 projects (supercritical water desalination through Ohio University and solvent-based desalination through Research Triangle Institute) are also under evaluation as to their cost, pilot readiness, utilities requirements, and footprint requirements; however, are not reported herein.

The assumptions and costs for each alternate high-TDS desalination technology are described in more detail below.

Forward Osmosis

Forward osmosis (FO) uses the spontaneous diffusion of water across a semipermeable membrane into a high salinity draw solution from a relatively lower salinity feed solution. Subsequent reconcentration of the diluted draw solution generates pure water product and concentrated draw solution for recycle to the FO unit. Figure 12 shows a schematic of an FO system. Draw solution regeneration can be conducted using thermal processes (e.g., steam stripping). Dissolved solids (e.g., NaCl) from the raw brine feed that are not rejected by the FO membrane appear in the draw solution stripping column bottoms product. In a pilot FO study, Oasys Water, Inc. utilized RO as a polishing step on this product to yield 300 mg/L TDS in the product water (McGinnis, 2013).

Although FO does not require hydraulic pressure, the energy requirements of draw solution regeneration are significantly greater than those of a standard RO desalination system, as will be shown below. The use of ammonium bicarbonate-based draw solutions is attractive due to the potential for NH_3 and CO_2 recovery with moderate heating. At temperatures of about 60^oC and above, ammonium bicarbonate decomposes to ammonia and carbon dioxide gases, which can be removed from the product water using vacuum steam stripping (McCutcheon, 2005). The absence of hydraulic pressure is expected to make FO membranes less prone to fouling by particulates than RO membranes, which may render the FO pretreatment requirements less stringent than RO pretreatment requirements.

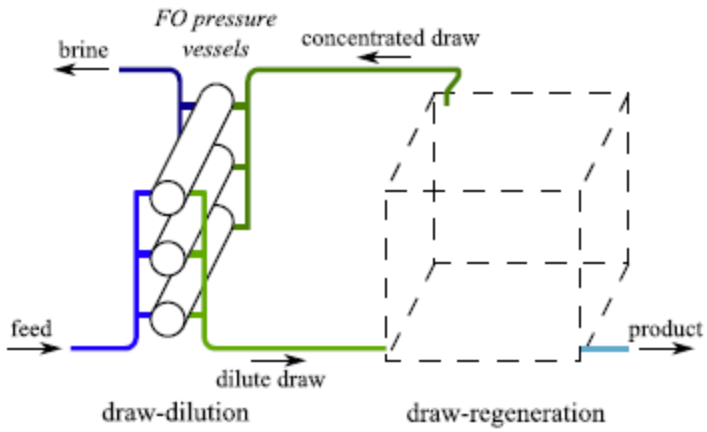

Figure 12. Schematic of FO Desalination System (McGovern & Lienhard, 2014)

Table 13 shows the design and operating parameters for FO desalination for both the design case and the Oasys Water, Inc. pilot study (McGinnis, 2013). Both cases utilize the same concentrated draw solution concentration (6 M CO_2 equivalent), but the feed and concentrate salinities for the design case are significantly higher than those of the Oasys case. The end conditions of the FO membrane flow rates were kept within the bounds recommended in the Oasys pilot report (McGinnis, 2013), which enabled calculation of the log-mean concentration driving force for water transport across the FO membrane. Assuming the FO membrane permeance calculated from the Oasys operating data applies to the design case, the membrane area was calculated for the design case.

Table 14 shows the cost-related parameters for this study. Table 15 shows the cost calculations for two cases, which differ by the energy source for the steam stripper that is used to reconcentrate the draw solution. Case 1 uses thermal energy (e.g., steam) for the draw solution stripping tower. At $6.00/MMBTU for heat, the cost of energy for draw solution regeneration is significant, making Case 1 more expensive than the base case (FF-MVR).

Table 13. FO Design and Operating Parameters

Parameter	Units	Design Case	Oasys Pilot
Raw feedwater rate	m^3/hr	113.55	0.229
Raw feed TDS	mg/L	180,000	73,000
Feed brine molarity	mole NaCl equiv/L	3.056	1.26
Raw feed density	gm/cc	1.1171	1.0486
gm H_2O in feed brine/mL feed brine	gm/mL	0.9371	0.976
Concentrate TDS	mg/L	295,000	180,000
Brine concentrate molarity	mole NaCl equiv/L	5.085	3.06
Concentrated brine density	gm/cc	1.1874	1.1171
gm H_2O in concentrate/mL concentrate	-	0.892	0.937
Concentrated brine flow rate	m^3/hr	69.28	0.093
Water recovered as product (permeate)	m^3/hr	44.58	0.14
Conc draw rate/brine feed rate	-	1.00	0.56
Conc draw solution flow rate	gpm	500	0.562
Conc draw solution, NH_4^+ salts	M, as CO_2 equiv	6.00	6.00
Dilute draw solution flow rate	gpm	696.3	1.16
Dilute draw solution concentration	M, as CO_2 equiv	4.31	2.90
Q=volumetric flow rate			
Q_brine feed/Q_Draw dilute	-	0.718	0.87
Q_brine concentrate/Q_Draw concentrate	-	0.61	0.73
Log-mean driving force	mole/L	1.07	2.23
Apparent membrane flux (Oasys pilot)	gfd		1.35
Apparent permeance (Oasys pilot)	gpm/(mole/L-ft^2)		0.00042
Membrane area	sq ft	433,540	639
Number of FO elements	-	2016	3
Membrane flux	gfd	0.65	1.35

Case 2 uses an electrically-driven MVR to supply energy to the draw solution stripping tower. Based on the Oasys pilot report (McGinnis, 2013), the electrical energy requirement for driving the MVR is 21 KWH_e/m^3 product water, as shown in Table 14. Even though electricity is five times more costly per KWH than heat, the amount of energy required for the MVR case is an order of magnitude lower than for Case 1, resulting in a significantly lower energy cost than Case 1. There is a cost penalty to the MVR case because it requires a vapor compressor. Despite the additional cost of the vapor compressor, the cost of Case 2 is significantly lower than the base case (FF-MVR).

Table 14. Forward Osmosis Cost Parameters

Parameter	Units	Value
Draw solution regen heat (case 1: heat)	KWH_{th}/m^3 product H_2O	275[a]
Draw solution regen electricity (case 2: MVR)	KWH_e/m^3 product H_2O	21[a]
Thermal energy cost	$/$KWH_{th}$	$0.02[b]
Electrical energy cost	$/$KWH_e$	$0.10
FO membrane element replacement interval	years	4
Element Cost (215 ft^2 membrane area)	$	$500[c]
Cost of capital	% of installed CAPEX/year	10

[a] Reference: (McGinnis, 2013)
[b] equivalent to $6.00/MMBTU
[c] Estimated based on vendor quote

Table 15. Estimated Forward Osmosis Costs

	Units	Case 1	Case 2
Energy source for draw solution recovery	-	Heat	MVR
Energy usage @ 275 KW_{th}/m^3 product water	KW	12,259	-
Energy usage @ 21 KW_e/m^3 product water	KW	-	936
Normalized energy cost	-	1.55	0.58
Normalized desal cost[a]	-	1.06	0.58

[a] (FO CAPEX + energy + membranes for FO)/(Base case CAPEX + electricity)

Membrane Distillation

Membrane distillation (MD) is a thermally driven membrane separation process that employs a vapor pressure gradient created between a warm saline feed solution and a cold distillate product separated by a hydrophobic microporous membrane. This membrane allows water vapor, but not liquid water, to permeate. Water evaporates on the feed side of the membrane, passes through the hydrophobic porous membrane and condenses on the cold distillate side, as shown in Figure 13. MD is not limited to low-TDS brine desalination; it has been tested on the pilot scale with saline streams approaching saturation (Silva J. , et al., 2014). Pretreatment to remove organics, particulates, and surfactants is required, as fouling and membrane wet out must be prevented to maintain good MD performance. MD is required to operate at sub-atmospheric pressures because the MD membrane operating temperature is limited. Low operating temperatures enable low-grade heat to be utilized as the primary heat source. Further, while MVR may be used for energy economy, sub-atmospheric pressure operation requires large vapor compressors and large ductwork, both of which add cost.

As with FO, there are two primary cases to consider for MD, based on the source of energy to heat incoming brine to the MD system. Case 1 utilizes heat, e.g., low pressure steam; Case 2 uses an MVR to recompress vapor distillate. The cost analysis for both cases is shown in Table 16.

Because an MD desalination system would be designed to operate at the same brine feed and concentrate compositions as the base case, the distillate and concentrate flow rates and compositions are the same for MD as for the base case. As with FO, the largest cost contributor to Case 1 is energy. If energy is available at a significantly lower cost than $6.00/MMBTU ($0.02/KWH$_{th}$), then MD could be cheaper than the base case (FF-MVR).

Table 16. MD Desalination Cost Comparison: Direct Heating vs. MVR

	Units	Case 1	Case 2
Energy source	-	Heat	MVR
Heat unit cost	$/KWH$_{th}$	$0.02[a]	-
Electricity unit cost	$/KWH$_e$	-	$0.10
Normalized desal cost[b]	-	1.03	0.86

[a] $6.00/MMBTU

[b] (MD CAPEX + energy + membranes + chemicals)/ (Base case CAPEX + electricity)

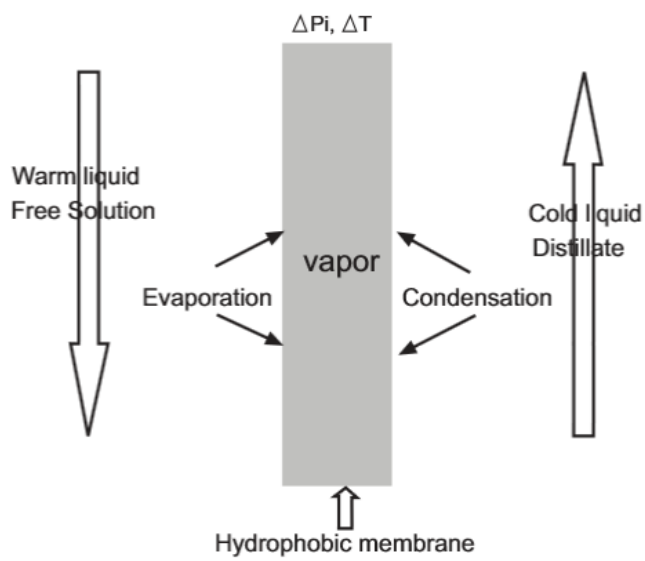

Figure 13. Membrane Distillation Schematic (Yarlagadda, Camacho, Gude, & Wei, 2009)

In 2013, GE, with partial funding from RPSEA contract 10122-07, conducted a successful field validation of MD for produced water recovery (Silva J. , et al., 2014). This project included a pretreatment system, membrane distillation modules, a vapor compressor, heat exchangers, and a measurement and control system. Most components were housed in a 20 foot shipping container. The system ran successfully for eight days continuously, with a maximum outlet brine concentration of 24 wt% (283 gm/L as NaCl). The distillate rate was 1 gpm (5 m^3/day), and the distillate had an average conductivity of <100 µS/cm.

Humidification-Dehumidification

In a recent article, several humidification-dehumidification (HDH) schemes were reviewed (Narayan, 2011). Under a GE-funded project, the GRC Oil & Gas Technology Center, in Oklahoma City, OK, has been developing a low-CAPEX HDH system for applications where low-cost energy is available (e.g., flare gas or waste heat from exhaust gas).

Figure 14 shows a simplified schematic representation of the proposed process. Hot carrier gas (pink) is generated using a gas-fired burner. The carrier gas heats brine (green) in a high-mass transfer rate humidifier in which water is evaporated from the heated brine. This water is recovered in the dehumidifier (blue). In the current design, the gas leaving the dehumidifier is vented to the atmosphere. Future designs may include gas recycle for heat recovery. Without energy recovery, the energy usage for this process is much higher than for MD, FO, or FF-MVR. However, if waste heat is available, this process may be attractive because of its low CAPEX.

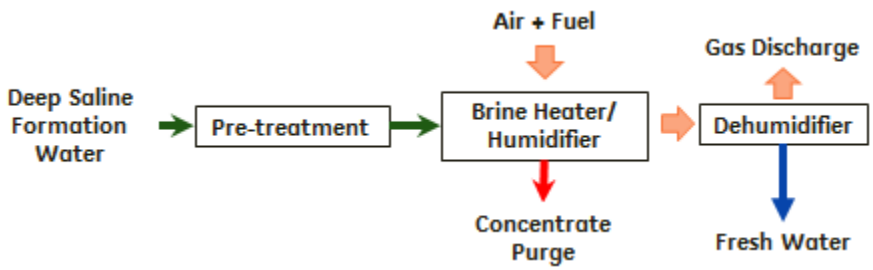

Figure 14. Schematic Diagram of Proposed HDH Desalination Process

The initial goals for piloting HDH are to identify ranges of gas and liquid flow rates that ensure efficient vapor-liquid mass transfer. Subsequent pilot trials will focus on heat integration. The feed, concentrate, and recovered water compositions and flow rates are the same for this process as for the base case. Case 1 utilizes propane as the heat source for the humidifier. Because no heat recovery is considered for the initial tests, the apparent cost of energy is artificially high. Case 2 utilizes waste heat (e.g., exhaust gas) for humidification. Table 17 shows the normalized cost of desalination for these two cases.

Table 17. HDH Normalized Cost Estimation

	Units	Case 1	Case 2
Energy source	-	Propane	Waste heat
Propane Lower Heating Value	BTU/lb	19,937	-
Energy cost (natural gas)	$/MM BTU	$6.00	-
Normalized energy cost[a]	-	3.55	-
Normalized CAPEX[b]	-	0.46	0.46
Normalized CAPEX + energy[c]	-	2.1	0.22

[a](HDH energy)/(Base case energy)
[b]CAPEX)/(Base case CAPEX)
[c] (HDH CAPEX + energy)/(Base case CAPEX + electricity)

Turbo-expander-based Freeze Desalination

Under a separate DOE-funded project, GE explored the use of multiphase turbo-expander technology for brine freeze desalination. This process is based on brine cooling by expansion of a mixed stream of compressed gas and brine in a turbo-expander. Although the turbo-expander concept may be applied to zero liquid discharge applications, for the BEST project analysis, it is assumed that the freeze desalination process yields ice and a brine concentrate. The ice is recovered as the pure water product. Thus, for this cost analysis, the feed, product, and concentrate stream flow rates and compositions are the same as for the base case.

Figure 15 shows a process flow diagram for a desalination process based on turbo-expander technology. As the gas stream expands in the turbo-expander, it cools and ice crystals are formed. These crystals are separated from the brine stream. Energy recovered from the expanding gas in the turbo-expander is used to partially offset gas compression energy requirements. For the gas stream, the process can utilize air or other gases. Table 18 shows the estimated normalized capital and energy costs for this process for base case operating conditions.

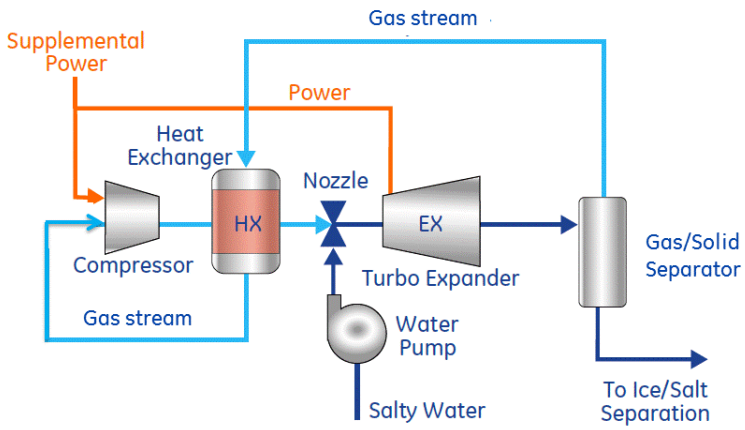

Figure 15. Process Flow Diagram: Desalination via Turbo-expander Technology

Table 18. Estimated Normalized Costs for Turbo-expander-based Freeze Desalination

	Normalized cost[a]
Energy	0.83
CAPEX	0.73
CAPEX + energy	0.78

[a](Cost)/ (Corresponding base case cost)

High Pressure Reverse Osmosis (HPRO)

Reverse osmosis (RO) has become the most common process for extracting pure water from saline water, constituting about 2/3 of worldwide installed capacity, outcompeting thermal processes due to its lower energy consumption and hence its lower cost compared to multi-effect distillation (MED) and Multi-Stage Flash (MSF) (Al-Karaghouli & Kazmerski, 2013).

This second function is relevant to the disposal of high salinity brines from Sea Water Reverse Osmosis (SWRO), shale gas produced waters, formation waters extracted during carbon dioxide sequestration, and flue gas desulfurization (FGD) water, all of which have high concentrations of dissolved solids compared to sea water and brackish water, the usual feeds for an RO process (see Table 19). Because a pressure in excess of the retentate's osmotic pressure must be applied to perform the separation, and because salt rejection increases with applied pressure, concentrating these solutions will require higher pressures than have been previously used (2400 – 5000 psi are considered, compared to 800-1000 psi for SWRO) (Baker, 2008). These increased pressures and more concentrated retentates create challenges regarding ion precipitation and scaling, biofouling, and RO module mechanical stability. Table 19 shows the typical composition of these high-pressure RO feed waters, the osmotic pressure after pretreatment, and the theoretical minimum retentate fractions that could be achieved using high-pressure RO at 2400 and 5000 psi.

Table 19. Properties of high-pressure RO feed waters

	SWRO brine[a] (50% recovery)	**Flowback water[b]**	**Formation water[c]**	**FGD wastewater[d]**
TDS [mg/L]	~72,000	~30,000 – 130,000	~5,000 – 300,000	~5,000-50,000
Δπ total [psi]	~800	~400-1200	~400 but can be much higher	~50 - 500
Δπ from monovalent salts [psi]	~750	~300 - 1100	~400 but can be much higher	~20 - 360
Major ions [symbol, mg/L]	Cl^- (20,000), Na^+ (11,000), Mg^{2+} (1300), K^+ (400)	Na^+ (13,000), Cl^- (12,000), Ca^{2+} (3600), HCO_3^- (1200), Sr^{2+} (1100), CO_3^{2-} (800), Br^- (300), K^+ (300), CO_2 (300), Ba^{2+} (200), Mg^{2+} (200), SO_4^{2-} (200)	Cl^-, Na^+ (~10,000 each), Ca^{2+}, Br^-, HCO3-, SO_4^{2-}, NO_3^-, Mg^{2+}, K^+ (100-1000 each)	Cl^- (1000-28,000), SO_4^{2-} (1500-8000), Mg^{2+} (1100-5000), Na^+ (700-5000), Ca^{2+} (750-4000), SiO_2 (70)
Min retentate fraction* (2500 psi)	0.3	0.12 to 0.44	0.16 or more	0.008 to 0.14
Min retentate fraction* (5000 psi)	0.15	0.06 to 0.22	0.08 or more	0.004 to 0.07

*The minimum retentate fraction corresponds to an ideal separation process, in which water permeation proceeds to equilibrium and in which concentration polarization, feed-side pressure drop, and membrane fouling are absent.

[a] = (Dickson & Goyet, 1994)

[b] = (Blondes, et al., 2016)

[c] = (Harto & Veil, 2011)
[d] = (Higgins, Sandy, & Givens, 2009)

A technoeconomic analysis of HPRO was also undertaken to compare it to the alternative technologies described above. Seawater RO concentrate was used as the design case feed (i.e., 70,000 mg/L TDS), and the design case flowrate was taken as 500 gpm. As shown in Table 20, high pressure reverse osmosis is energetically favorable compared to standard thermal brine concentration with falling film mechanical vapor recompression (FF-MVR). However, there are challenges associated with the high-pressure operation required to overcome the increasing osmotic pressure of the concentrated brine. Compared to seawater RO requirements, a more robust, compaction resistant membrane module is required, as well as a system that is high pressure and corrosion-resistant. Therefore, an effort to better understand CAPEX implications was undertaken.

Table 20. Normalized Energy Cost of High Pressure Reverse Osmosis

Concentrate TDS (mg/L)	Concentrate osmotic pressure (psi)	RO/FF-MVR energy cost
130,000	~1900	0.51
175,000	~2800	0.55
245,000	~4800	0.69

The overall costs of HPRO were calculated for four cases, using the final concentrate TDS values from Table 21 (130,000 mg/L, 175,000 mg/L, 245,000 mg/L and 295,000 mg/L TDS), and this cost was compared to the cost of the base case falling-film mechanical vapor recompression (FF-MVR) technology for each case. Figure 17 summarizes the four design cases studied for comparison of HPRO to base-case FF-MVR technology.

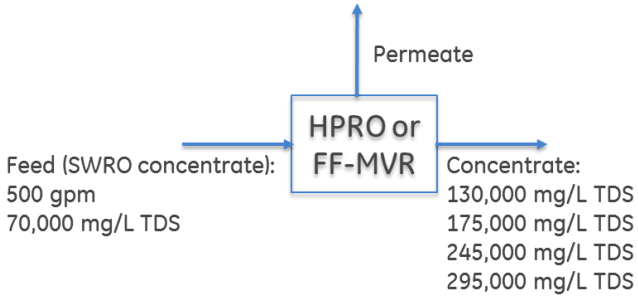

Figure 16. Design Cases for HPRO vs. FF-MVR Technoeconomic Analysis

The operating feed pressure for each design case is listed in Table 21. Operating pressure is calculated as the osmotic pressure of the final concentrate, plus a constant additional pressure to overcome the osmotic pressure and ensure flow through all elements.

Table 21. HPRO Feed Pressure and Concentrate Concentration

Final concentrate TDS (mg/L)	Feed pressure (psi)
130,000	2000
175,000	3000
245,000	5000
295,000	6800

HPRO equipment cost estimation was performed using a factored estimate approach, in which factors for time, material of construction, pressure requirement, and corrosion allowance are used to scale the base cost of the equipment. The final cost of the equipment (C_V) is given by Equation 1:

$$\boldsymbol{C_V = C_B F_t (B_1 + B_2 F_M F_P) F_C} \quad (1)$$

where C_B is the base cost of the equipment, F_t is the time index, F_M is the material of construction factor, F_P is the pressure factor, F_C is the corrosion factor, and B_1 and B_2 are constants that correlate costs of pressure and material choice for a particular type of equipment (Ulrich & Vasudevan, 2004). The F_M, F_P, and F_C factors are interrelated, since a pressure vessel wall thickness will be determined by the strength of the material (F_M), the pressure of the system (F_P) and the allowance in thickness for corrosion (F_C).

The time factor is simply the ratio of the Chemical Engineering Index for Plant Equipment Costs at the current time (I_{t2}) divided by the index and the time the base cost was determined (I_{t1}) (Chemical Engineering Plant Cost Index, 2016), as shown in Equation 2:

$$F_t = \frac{I_{t2}}{I_{t1}} \quad (2)$$

The material factor is the ratio of the cost of the desired material (F_{M2}) to the cost of the base material (F_{M1}), as shown in Equation 3:

$$F_M = \frac{F_{M2}}{F_{M1}} \quad (3)$$

Table 22 gives material factors for corrosion-resistant alloys (Rolled Alloys Relative Pricing, 2016).

Table 22. Material Factors for Corrosion-Resistant Alloys

Material	F_{Mi}

Carbon Steel	0.4
304 Stainless Steel (SS)	0.8
316 SS	1.0
Duplex SS	1.8
Austenitic SS	2.4
Super Austenitic SS	3.0
Alloy 20 (Ni/Cr/Mo SS)	3.5
Alloy 625 (Inconel)	6.3
Alloy C-276 (Hastelloy)	6.8
Titanium	9.4

Based on ASME code (American Society of Mechanical Engineers (ASME), International Boiler and Pressure Vessel Code (BPVC), Section VII; http://www.engineeringtoolbox.com/asme-boiler-vessel-code-d_8.html, May 24, 2017), the pressure factor for vessels is given by Equation 4:

$$F_{P,vessel} = \frac{\frac{(P+1)D}{2[850-0.6(P+1)]}+0.0315}{0.0063} \quad (4)$$

where P is the working pressure in bar(g) and D is the vessel diameter in meters.

For all other types of process equipment, the pressure factor is given by Equation 5:

$$log_{10}F_P = C_1 + C_2\, log_{10}P + C_3\, log_{10}P^2 \quad (5)$$

where P is the working pressure in bar(g) and C_1, C_2 and C_3 are constants based on pressure rating (0.03881, -0.11272, and 0.08183, respectively, for pressures between 5 and 140 bar(g)).

The corrosion factor is estimated with Equation 6:

$$F_C = \frac{w_t+CR_a t_l}{w_t+CR_s t_l} \quad (6)$$

where w_t is the base wall thickness, CR_s and CR_a are the standard and accelerated corrosion rates (mm/year), and t_l is the lifetime of the unit. The corrosion factor is an incremental cost for the extra material needed to produce the vessel, as typical fabrication costs will be similar.

Capex was calculated from equipment cost estimates using a 2x installation factor and a 10 year straight line depreciation or payback period. Opex was calculated from pumping power requirements for the required feed pressures in Table 21, and an electricity cost of $0.10/kWh. The normalized (HPRO vs. FF-MVR) Capex + Opex costs for the four design cases are summarized in Table 23.

Table 23. Normalized Cost of HPRO

Final concentrate TDS (mg/L)	Normalized Capex + Opex*
130,000	0.31
175,000	0.32
245,000	0.39
295,000	0.38

*Normalized cost = HPRO cost/FF-MVR cost; cost per m^3 product water

As shown in Table 23, HPRO is estimated to cost approximately 1/3 the cost of the base case FF-MVR technology. The seawater RO concentrate design cases studied here suggest that if HPRO were technically feasible, it would be a valuable technology for high TDS desalination. Significant technical challenges exist for HPRO, however, including the ability to operate RO elements at the required feed pressures, membrane performance at high pressure, and scaling and fouling concerns due to the feed concentrations and compositions that will be encountered by the HPRO membranes.

The high TDS desalination technologies' costs (Capex, energy and consumables such as chemicals or membranes) are compared to the base case FF-MVR technology cost, as summarized in Table 24.

Table 24. Normalized Cost of High TDS Desalination Technologies

Technology	Estimated normalized cost per m^3 product water*
FF-MVR	1.0
Humidification-dehumidification (HDH) with natural gas	2.1
Membrane distillation (MD) with MVR	0.85
Turboexpander-freeze	0.77
Forward osmosis (FO) with MVR	0.58
Solvent extraction	0.35
High pressure reverse osmosis (HPRO)	0.31-0.39[#]

*Normalized cost = high TDS technology cost/FF-MVR cost;

[#] Costs vary based on concentrate TDS (mg/L), application space

Two additional cases were considered, in seawater and flue gas desulfurization wastewater applications. While seawater RO concentrate (i.e., ~70,000 mg/L total dissolved solids, or TDS) was used as the design case feed for seawater applications in the previously presented technoeconomic analysis, seawater (i.e., ~35,000 mg/L TDS) was used as the design case feed here. The cost of a hybrid seawater RO (SWRO) plus HPRO system was compared to that of a standard SWRO system made twice as large to achieve the same total pure water recovery rate

as the hybrid SWRO + HPRO system. Figure 17 illustrates the base case (2x SWRO system) and Figure 18 summarizes the four cases studied for comparison of the hybrid SWRO + HPRO system to the base case 2x SWRO system. Case (a) uses a standard-size SWRO system (445 gallons per minute (GPM) of 35,000 mg/L TDS feed with 200 GPM of permeate and 245 GPM of 63,000 mg/L TDS concentrate produced), which requires the second stage HPRO system to concentrate to 295,000 mg/L TDS to produce 200 GPM of permeate, for a total of 400 GPM permeate from the hybrid system. Cases (b) through (d) use larger SWRO systems, which produce more of the total permeate volume, relaxing the permeate production demand on the second stage HPRO system, which translates to lower final concentration requirements for the HPRO unit. The operating pressures required for the HPRO system in each of the four cases shown in Figure 18 are reported in Table 21. Operating pressure is calculated as the osmotic pressure of the final concentrate, plus a constant additional pressure to overcome the osmotic pressure and ensure flow through all elements.

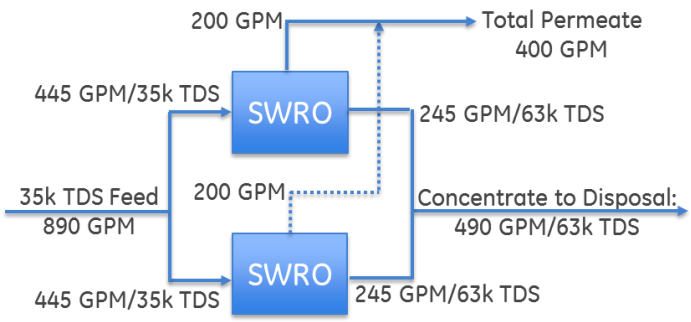

Figure 17. Base Case 2x SWRO System for Comparison to Hybrid SWRO + HPRO System

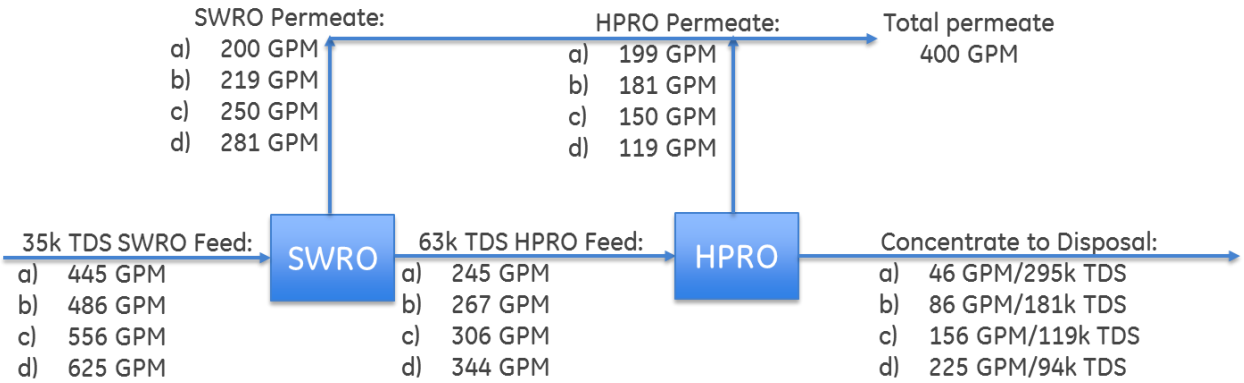

Figure 18. Hybrid SWRO + HPRO System Cases Studied

Costs included in the technoeconomic analysis included Capex, energy and membrane replacement for the SWRO and/or HPRO units, as well as pretreatment and concentrate disposal costs. HPRO equipment cost was calculated using the factored estimate approach

reported previously, and SWRO equipment cost was estimated by scaling the known cost of a standard system to the larger system sizes required. Capex was then calculated from the equipment cost estimates using a 2x installation factor and a 10-year straight line depreciation or payback period. Energy cost (Opex) was calculated from pumping power requirements for the required feed pressures in Table 21, and an electricity cost of $0.10/kWh. Membrane replacement was calculated using known SWRO element cost and a predicted lifetime, with HPRO elements assumed to cost twice as much and to have ¼ the lifetime of SWRO elements. Industry-standard SWRO pretreatment costs were used, with multipliers for HPRO depending on the concentrate TDS required (i.e., higher concentrate TDS will require more extensive pretreatment to prevent fouling, scaling, etc.). Concentrate disposal cost was estimated as the cost of constructing a new ocean outfall with diffusers for the required concentrate volumes.

Table 25 shows the normalized cost of the hybrid SWRO + HPRO systems depicted in Figure 18. In each case, the hybrid SWRO + HPRO system cost is normalized to that of the base case 2x SWRO system depicted in Figure 17. The hybrid system is estimated to cost ~10-25% less than the base case SWRO system, but, perhaps unexpectedly, cost is not minimized by pushing the HPRO unit to the highest possible concentrate TDS (i.e., case (a) is not the cheapest). This is due to changing percent contributions of Capex, electricity (or energy, Opex) and concentrate disposal as the system is made larger (i.e., higher SWRO + HPRO Capex and concentrate disposal costs) to reduce the required concentrate TDS from the HPRO unit (i.e., lower required feed pressure and energy use), as shown in Figure 19. As a comparison, the base case 2x SWRO system cost breakdown is 12% Capex, 34% electricity, 48% concentrate disposal, 5% pretreatment, and 1% membrane replacement. Table 25 and Figure 19 show that the potential cost savings of a hybrid HPRO + SWRO system are situation-dependent, and the circumstances of a given installation (e.g., available footprint, distance to disposal, energy availability and cost) will determine the optimal balance between system size and extent of concentration required of the HPRO unit to realize the maximum savings potential.

Table 25. Normalized Cost of Hybrid SWRO + HPRO System Cases Studied

Case	System Feed Flowrate (GPM)	System Concentrate Flowrate (GPM)	System Concentrate TDS (mg/L)	Normalized Cost*
(a)	445	46	295,000	0.90
(b)	486	86	181,000	0.76
(c)	556	156	119,000	0.82
(d)	625	225	94,000	0.91

*Normalized cost = (hybrid SWRO + HPRO system cost)/(2x SWRO system cost); cost per m^3 product water

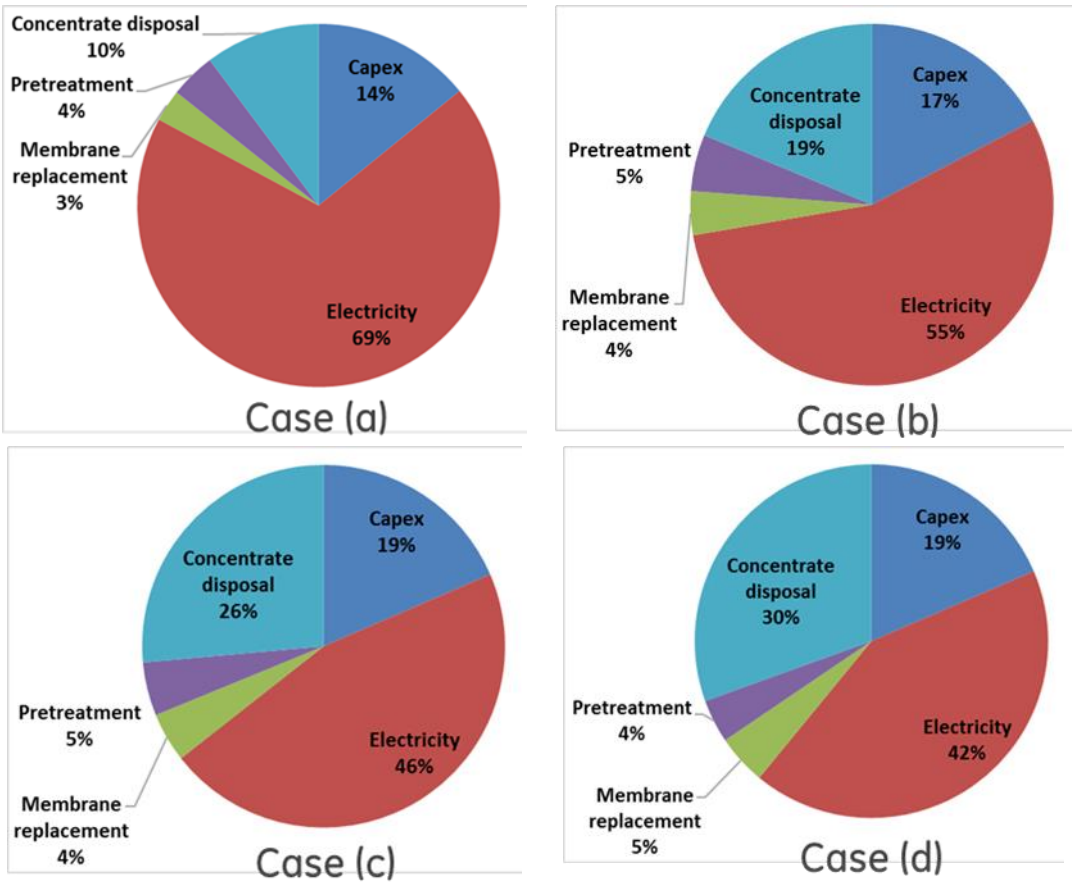

Figure 19. Cost Breakdown of Hybrid SWRO + HPRO System Cases

The second application studied was flue gas desulfurization (FGD) wastewater treatment. Although flue gas desulfurization wastewater typically contains high levels of sodium, magnesium, calcium, chloride and sulfate [1,2], a sodium chloride feed (40,000 mg/L TDS, 500 GPM) was used as the design case, with consideration for the scaling potential of FGD wastewater accounted for with pretreatment (i.e., softening). Figure 20 illustrates the base case falling-film mechanical vapor recompression (FF-MVR) plus crystallizer (XTL) system for FGD wastewater treatment (FGD wastewater treatment is typically a ZLD application), and Figure 21 summarizes the five cases using RO preconcentration (SWRO or SWRO + HPRO) before the FF-MVR and/or XTL that were compared to the base case. In each of the five cases and the base case, the same total amount of product water was produced (488 GPM). Case 1 uses only standard SWRO preconcentration before the FF-MVR and XTL units, while cases 2-5 use SWRO and a second stage HPRO unit before evaporation and/or crystallization. The size of the FF-MVR and/or XTL units vary with the extent of RO preconcentration in each case. Depending on the concentrate TDS reached by the HPRO unit, a FF-MVR may not be needed before the XTL (i.e., if the HPRO concentrate TDS is high enough, the concentrate can be sent directly to a XTL). For Cases 2 and 3, a FF-MVR and XTL are used, while for Cases 4 and 5, the HPRO concentrate is sent directly to the XTL. The HPRO concentrate TDS is identical in Cases 3 and 4 (175,000 mg/L), allowing comparison of the downstream two unit (FF-

MVR + XTL) and single unit (XTL) options. The operating pressures required for the HPRO unit in each of the cases shown in Figure 21 are summarized in Table 26.

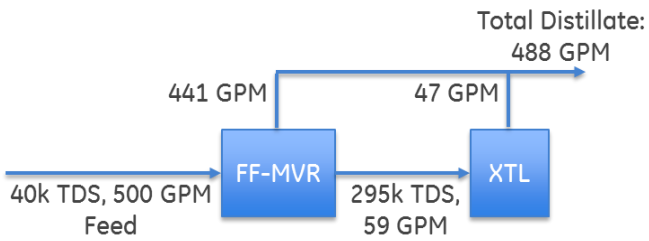

Figure 20. Base Case FF-MVR + XTL FGD Wastewater Treatment System

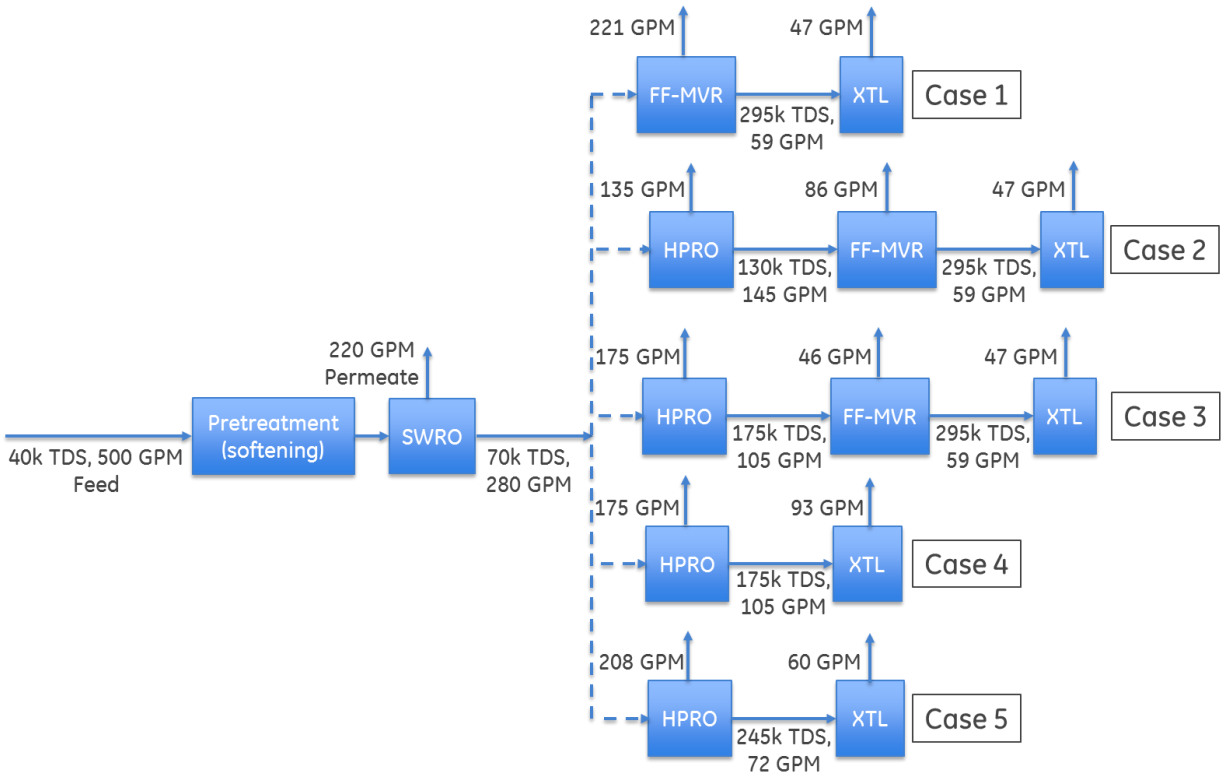

Figure 21. RO Preconcentration (SWRO or SWRO + HPRO) FGD Wastewater Treatment Cases Studied

Table 26. HPRO Feed Pressure and Concentrate Concentration

Case	HPRO Concentrate TDS (mg/L)	HPRO Operating Pressure (psi)
2	130,000	2000
3,4	175,000	3000
5	245,000	4900

Costs included in the technoeconomic analysis included Capex and energy (electricity) for the desalination units (SWRO, HPRO, FF-MVR and XTL), membrane replacement for the SWRO and/or HPRO units, as well as RO pretreatment (i.e., softening, to address scaling concerns for FGD wastewater). The base case FF-MVR + XTL ZLD technologies are much more robust to scaling than membrane technologies, and therefore do not require softening. The costs of other pretreatment (i.e., total suspended solids, or TSS) and sludge disposal (i.e., TDS sludge from XTL) were not included because they are expected to be the same in all cases (base case and Cases 1-5). Costs were calculated using the same methods described above for the seawater application.

Table 27 shows the normalized cost of the five cases depicted in Figure 21 using RO preconcentration (SWRO or SWRO + HPRO) before the FF-MVR and/or XTL. In each case, the cost is normalized to the cost of the base case FF-MVR + XTL system depicted in Figure 20. Preconcentration with standard SWRO alone before the FF-MVR + XTL (i.e., Case 1) is estimated to save ~10% compared to the base case without RO preconcentration, however the savings for systems employing SWRO and HPRO preconcentration (Cases 2-5) are much larger (up to ~40%), demonstrating the economic benefit of HPRO technology in this ZLD application. The cost savings for Cases 3 and 4 are very similar, suggesting the choice of a FF-MVR + XTL (Case 3) or XTL alone (Case 4) will be more dependent on other considerations, such as available footprint.

Table 27. Normalized Cost of RO Preconcentration (SWRO or SWRO + HPRO) FGD Wastewater Treatment Cases Studied

Case	Normalized Cost*
1	0.87
2	0.65
3	0.62
4	0.66
5	0.58

*Normalized cost = (FGD wastewater treatment with RO pretreatment system cost)/(FF-MVR + XTL system cost); cost per m^3 product water

3. Task 4: Pre-pilot process validation

a. Pre-piloting of promising pretreatment technologies

GRC received 19 totes (275 gal/tote) each of Bakken and Eagle-Ford production water for pre-pilot scale testing of four GE-developed pretreatment technologies: micro-clarification, which is a novel approach to solid-liquid separation and has potential to significantly reduce the footprint requirements for clarification, membrane microfiltration, which utilizes microporous ePTFE with either a hydrophilic coating or a hydrophilic-oleophobic coating to avoid fouling by

oily particulates, oil-rejecting ultrafiltration, and a steam-regenerable adsorbent, which has potential for cost reduction. Each of these technologies may be tested on a slipstream in the BEST pilot pretreatment system.

Key pilot-ready technologies identified for extracted water pretreatment are shown in Table 28. Technoeconomic modeling for microclarification (MC), oil-tolerant microfiltration (MF) and steam regenerable sorbent (SRS) technologies was also conducted.

Table 28. Pilot-ready Extracted Water Pretreatment Technologies

Technology	Target impurities	Advantage
Micro-clarification (MC)	Particulates > 5 µm	Low footprint vs. clarifier Cost parity with clarifier
Oil-tolerant microfiltration (MF)	Particulates > 1 µm	Low fouling, lower cost vs. clarifier
Oil-rejecting ultrafiltration (UF)	Particulates > 0.01 µm Free, emulsified oils	Unique product, field-proven
Steam regenerable sorbent (SRS)	Dissolved organics	Low-cost vs. existing commercial sorbents

Microclarification

GE's new microclarifier (MC) technology utilizes shallow channels to optimize settling and reduce clarification times from hours to about 90 seconds. Microclarification technology, which has the potential to reduce footprint by about a factor of 5 compared with a conventional clarifier, works by ensuring laminar flow along the flow path, which optimizes flow dynamics for efficient settling, and by minimizing settling height along the channel. This system can reliably reduce feed turbidity from greater than 1000 NTU to less than 50 NTU (often less than 10 NTU) for field-sourced produced waters.

The main driver in MC cost is the residence time required in the channels, which is a function of particle size (smaller, less dense particles require longer settling times). The particle size used in MC cost modeling was chosen based on analysis of Bakken field production water. The cost of MC was determined to be roughly the same as that of conventional lamella clarifier technology. The main advantage of MC over conventional technology is the reduced footprint of MC.

A 1-gallown per minute MC system was tested with synthetic extracted water. Figure 22 shows a photograph of a single channel of a microclarification stack. Figure 23 shows the performance of the microclarifier prototype on field-sourced water.

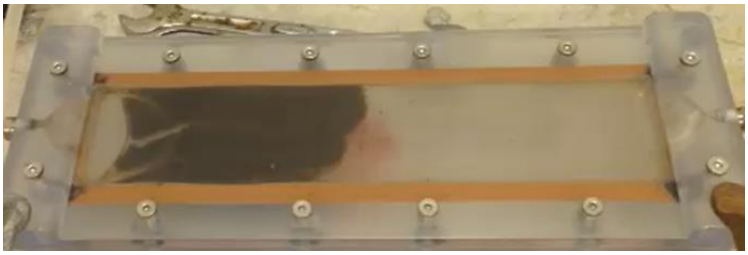

Figure 22. Single Channel Microclarifier Prototype

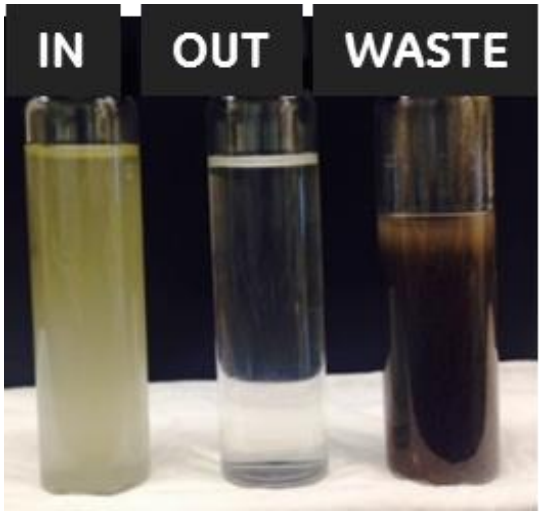

Figure 23. Microclarifier Performance with Field-sourced Produced Water

Figure 24 shows the prototype microclarification unit in GRC's pretreatment pre-pilot test facility. Figure 25 shows the feed, effluent (clarate), and purge streams processed with the prototype microclarifier, for experiments conducted using Bakken and Eagle-Ford production waters as feed to the unit. This system can reliably reduce feed turbidity from hundreds of NTU to less than 50 NTU for field-sourced production waters.

Figure 24. Prototype Microclarification Unit

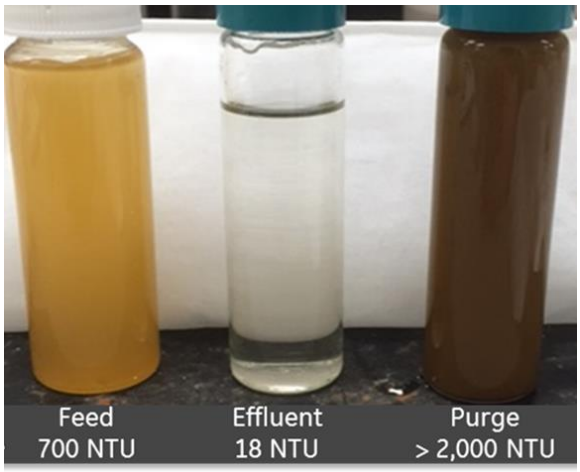

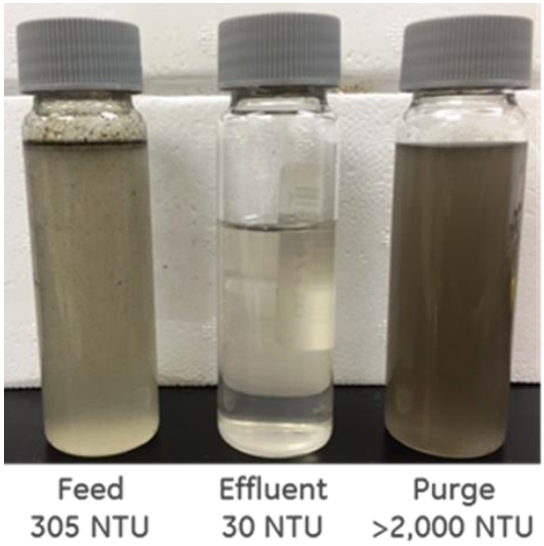

(a) **(b)**

Figure 25. Prototype Microclarifier Performance with (a) Bakken and (b) Eagle-Ford Production Water.

Oil-tolerant Microfiltration Membranes

Oil-tolerant microfiltration (MF) technology requires the same equipment as conventional MF (e.g., pumps, housings, skid). The only difference is the membrane used, with a fouling-resistant coating being applied in the case of oil-tolerant MF. The coated membrane cost is nominally the same as that of conventional MF membranes. Therefore, the CAPEX for oil-tolerant MF is approximately the same as that of conventional MF. Reduced backwash frequency and membrane replacement (i.e., reduced OPEX) are projected benefits of oil-tolerant MF technology. Extended lifetime testing remains to be performed to quantify these benefits.

Microfiltration tests were conducted on a 0.5 gpm scale with a synthetic produced water, which was spiked with a standard clay. The control membrane filter was a commercially available, hydrophilic ePTFE microfilter (GEPW OnePass™, uncoated). The test membrane filter was the same material, but coated with a patented hydrophilic, oleophobic coating.

Each filter was operated under constant flux during a service cycle. The filter was backwashed with deionized water after the transmembrane pressure exceeded a predetermined threshold. After each backwash the transmembrane pressure was recorded. The extent to which the post-backwash transmembrane pressure increases with each cycle is indicative of membrane fouling. These tests were run on a 12” long x 3” diameter candle filter shown in Figure 26.

Figure 26. Candle Filter used in 0.5 gpm Tests

Figure 27 compares the beginning-of-cycle (after backwash) trans-membrane pressure for both uncoated and coated membrane filters as a function of the cumulative solids loading onto the filter. The abscissa is a measure of the cumulative foulant load (oily clay particles) that the membrane filter has processed. Symbols represent the measured transmembrane pressure after the backwash at the end of each service-backwash cycle. This plot shows that the membrane coating is effective in preventing membrane fouling.

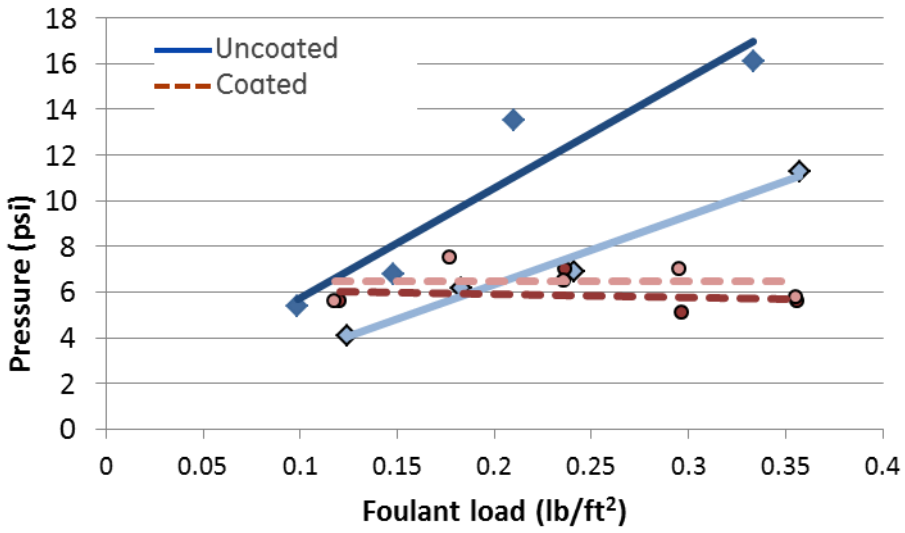

Figure 27. Performance Comparison: Coated (oil-tolerant) vs. Uncoated Microfiltration Membranes with Synthetic Produced Water

The coating was applied to these 12" long candle filters by spray coating. A roll-to-roll process was developed and tested for a dip-coating process; this process was scaled up in a manufacturing environment to yield hundreds of linear yards of coated membrane material. Samples of this coated material were laminated to a backing, made into candle "socks", and tested in the GEGR pretreatment facility at 2 gpm.

Figure 28 shows GRC's 2 gpm pre-pilot microfiltration (MF) unit with automated backwash capability. Figure 29 shows the performance of a backwashable microfilter for a series of cycles (filtration followed by backwash). This test was performed on the GRC pre-pilot unit, using commercially available MF membranes and Bakken production water diluted to 180 gm/L TDS. For each cycle, the filter was operated at constant flux, and the backwash was triggered on the transmembrane pressure (TMP) reaching approximately 20 psi. The TMP was also measured with a constant flux of deionized (DI) water before (5 psi) and after (6.9 psi) this series of five filtration and backwash cycles, as shown in Figure 29. Although more filtration cycles are needed to define the cleaning interval and filter element lifetime for a specific feed water, these results are promising.

Figure 28. Microfiltration Unit in GRC Pre-pilot Facility

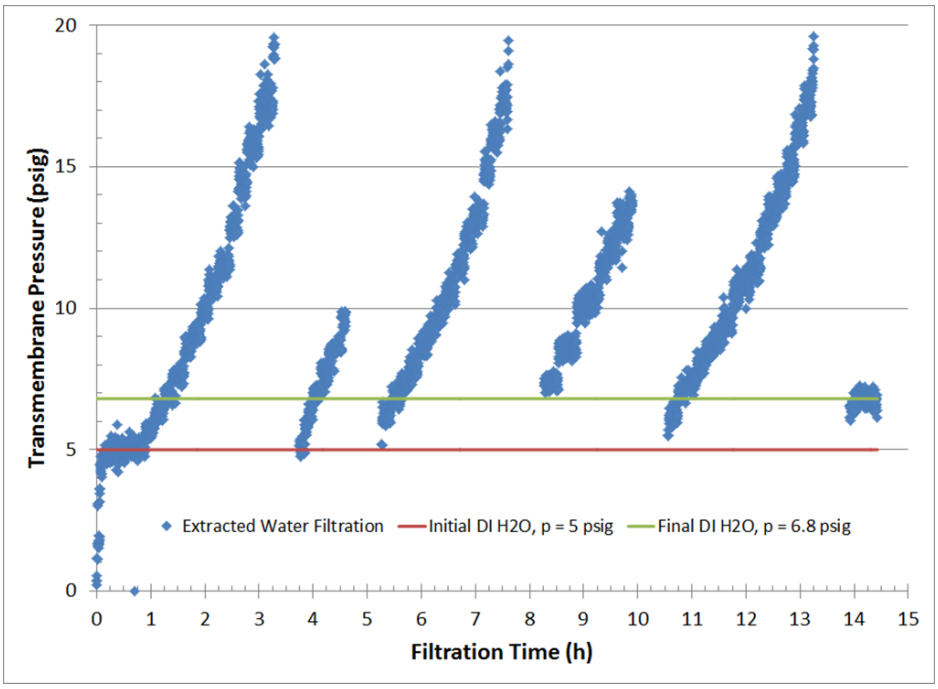

Figure 29. Microfilter Performance with Bakken Production Water

Oil-rejecting Ultrafiltration

A GE E4 reverse osmosis test system was modified to accommodate ultrafiltration elements. Three spiral-wound GEPW M-Series oil-rejecting UF modules are configured in series. Figure 30 shows a diagram of a typical spiral-wound membrane filter element.

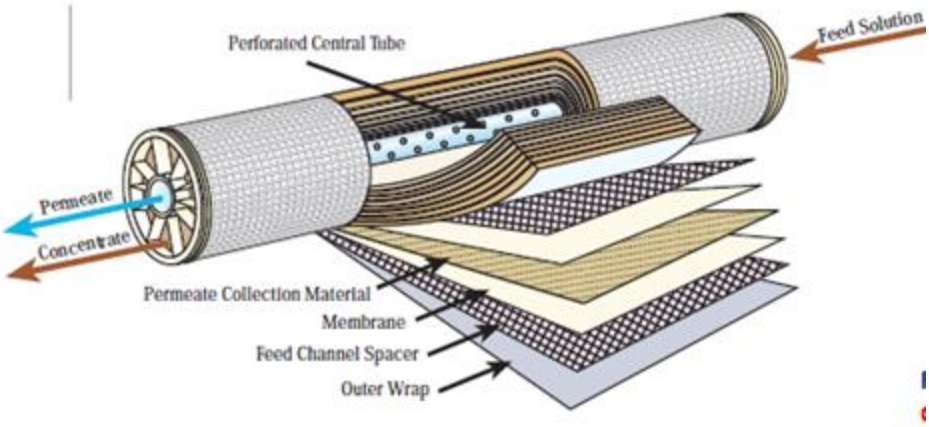

Figure 30. Schematic Diagram of Spiral-wound UF Element

Figure 31 shows photographs of two sample vials. The vial on the left contains raw field produced water that contained a significant amount of free oil. The photograph on the right shows the material leaving the M-Series UF system.

Figure 31. Photographs of Sample Vials Before and After M-Series UF Pretreatment

All brine that has undergone microfiltration is also filtered in a skid-mounted ultrafiltration (UF) system, shown in Figure 32. The UF membrane modules were in service for approximately 5 months with no apparent decrease in performance.

Figure 32. Ultrafiltration Unit in GRC Pre-pilot Facility

Steam-regenerable Sorbent

A key unit operation in GEGR's pretreatment facility is a 4" x 36" column for testing steam-regenerable sorbents (SRS) with field and synthetic brines. GEGR synthesized a batch of proprietary SRS resin. This resin has been loaded into the SRS column and conditioned with steam for several hours. This unit has been utilized to treat several hundred gallons of spiked field produced water.

Like oil-tolerant MF, GE's steam regenerable sorbent (SRS) technology uses the same equipment as existing sorbent technologies, so CAPEX will be nominally the same. Improvement in sorbent lifetime (time to regeneration, number of regeneration cycles), the main contributor to OPEX, could reduce the cost of GE's SRS technology relative to existing sorbent technologies, but extended lifetime testing is needed to complete the cost comparison.

GE has tested both commercial and developmental steam-regenerable sorbents (SRS for removing organics from brine streams. Figure 33 shows GRC's pre-pilot steam regenerable sorption unit, including the 4" x 36" column for testing adsorbents and the steam generator.

(a) **(b)**

Figure 33. Steam-regenerable Sorption Unit in GRC Pre-pilot Facility: (a) Resin Column and (b) Steam Generator

Figure 34 shows the performance of a developmental synthetic adsorbent for three feed compositions. The feed comprised production water either as received, or as spiked with toluene, which was used as a surrogate for benzene, toluene, ethyl benzene, and xylene (BTEX). For both the high and moderate organics feed cycles, the normalized toluene concentration in the SRS-treated water shows negligible leakage, followed by a relatively steep breakthrough. For the low organics feed, the effluent showed non-detectable toluene through 1600 bed volumes of feed.

Between adsorption cycles, the resin was regenerated by feeding approximately 160°C steam to the column. Figure 35 shows typical results for steam regeneration. The bulk of the organics are removed within 30 minutes of starting the regeneration.

To date, this developmental adsorbent has undergone six adsorption-regeneration cycles and processed over 5,000 gallons of field produced water. Based on these pre-pilot results, the developmental SRS is a candidate for inclusion in Phase 2 pilot testing.

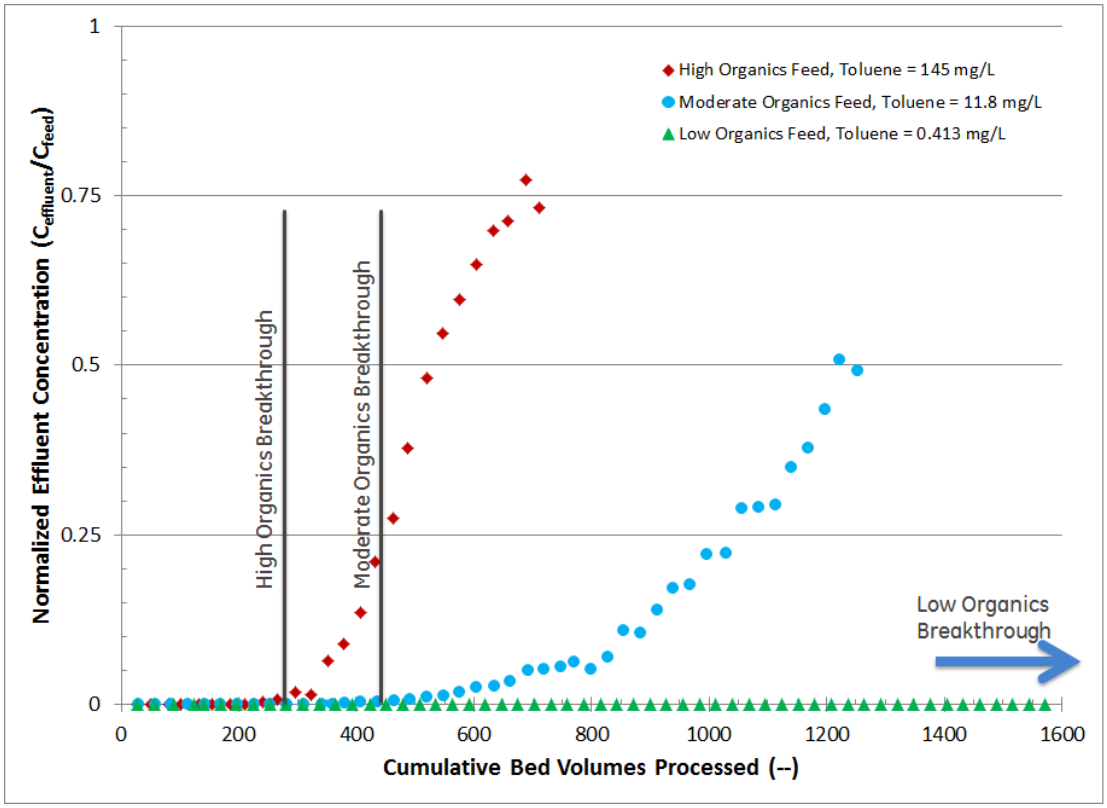

Figure 34. Toluene Breakthrough Curves for Steam Regenerable Sorbent

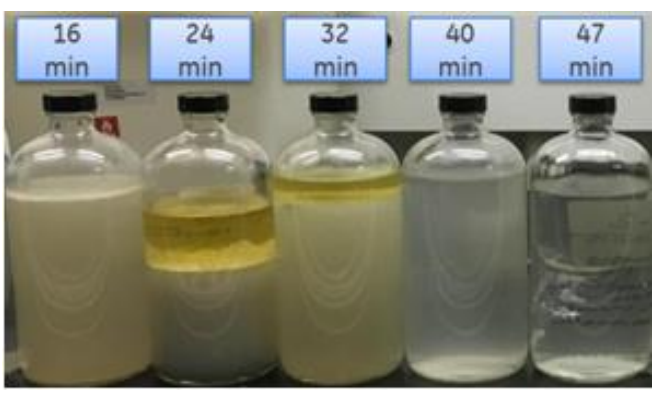

Figure 35. Condensate Recovered During Steam Regeneration

b. <u>Pre-piloting of promising desalination technologies</u>

Brine Concentrator Process Validation

An Aspen Plus model of a brine concentrator was developed to identify the maximum concentration factor (CF) that can be used for a given extracted water composition without crystallization of NaCl or other salts. Figure 36 shows the calculated temperature as a function of concentration factor in a brine concentrator for Bakken production water that has

undergone minimal pretreatment (organics and suspended solids removal only). For this water, the maximum concentration factor without NaCl precipitation is about 1.8.

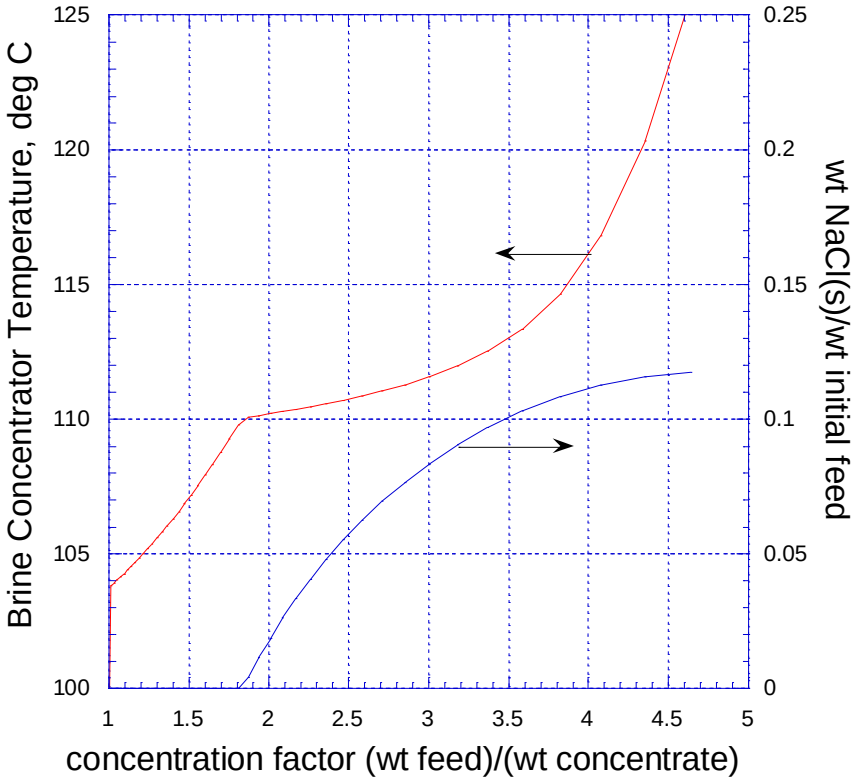

Figure 36. Brine Concentrator: Onset of NaCl Crystallization

The components identified as critical for HPRO operation are circled in the schematic of a standard RO element (Spiral-wound reverse osmosis element configuration, 2017) shown in Figure 37. Changes to the perforated central tube and permeate collection material demonstrated the ability to improve compaction resistance to some degree, but improvements in the membrane itself were determined necessary to achieve further improvement in element performance at high pressure.

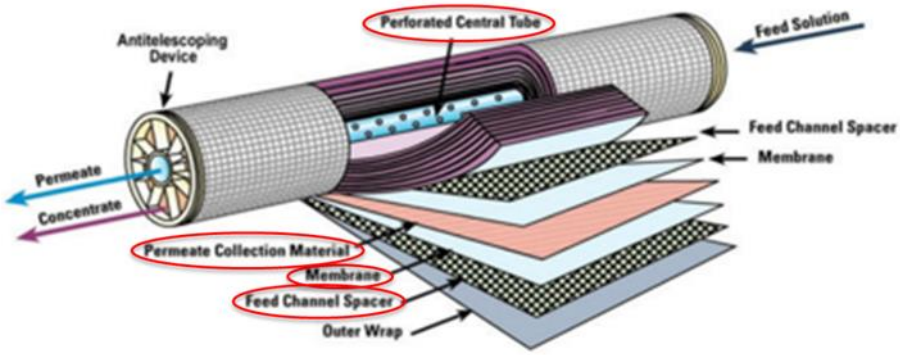

Figure 37. Reverse Osmosis Element Configuration

The RO membrane is a composite material, composed of a thin film polyamide separating layer polymerized on a polysulfone ultrafiltration membrane support. The ultrafiltration layer is porous and is likely a source of much of the compaction observed in HPRO operation.

4. Pilot System Conceptual Design

Figure 38 shows a conceptual design for the pretreatment portion of the BEST desalination system. Quotes are in hand for most major equipment items. GEGR has contacted the engineering manager of GEPW's field pilot design team to leverage their expertise in developing plans to define a field pilot system. Depending on the composition of field samples received, an optional deoiling section may need to be installed upstream of this pretreatment system.

The base case high-TDS desalination system is a falling film evaporator with mechanical vapor recompression (FF-MVR). This technology is commercial, with about 100 units installed worldwide in a variety of desalination applications, including cooling tower blowdown recovery and flue-gas desulfurization water recovery. To economically validate this technology for extracted water under Phase 2, we plan to pretreat extracted water in the field BEST pilot system, and ship the pretreated water to GE's pilot facility in Bellevue, Washington for a 3-4 week trial. This approach is significantly more cost-effective than building a dedicated FF-MVR system for the field trial.

Work is underway to define the utilities required for a 3 gpm HDH desalination system, which is currently the leading alternative high TDS desalination technology under consideration for comparison against the base case FF-MVR.

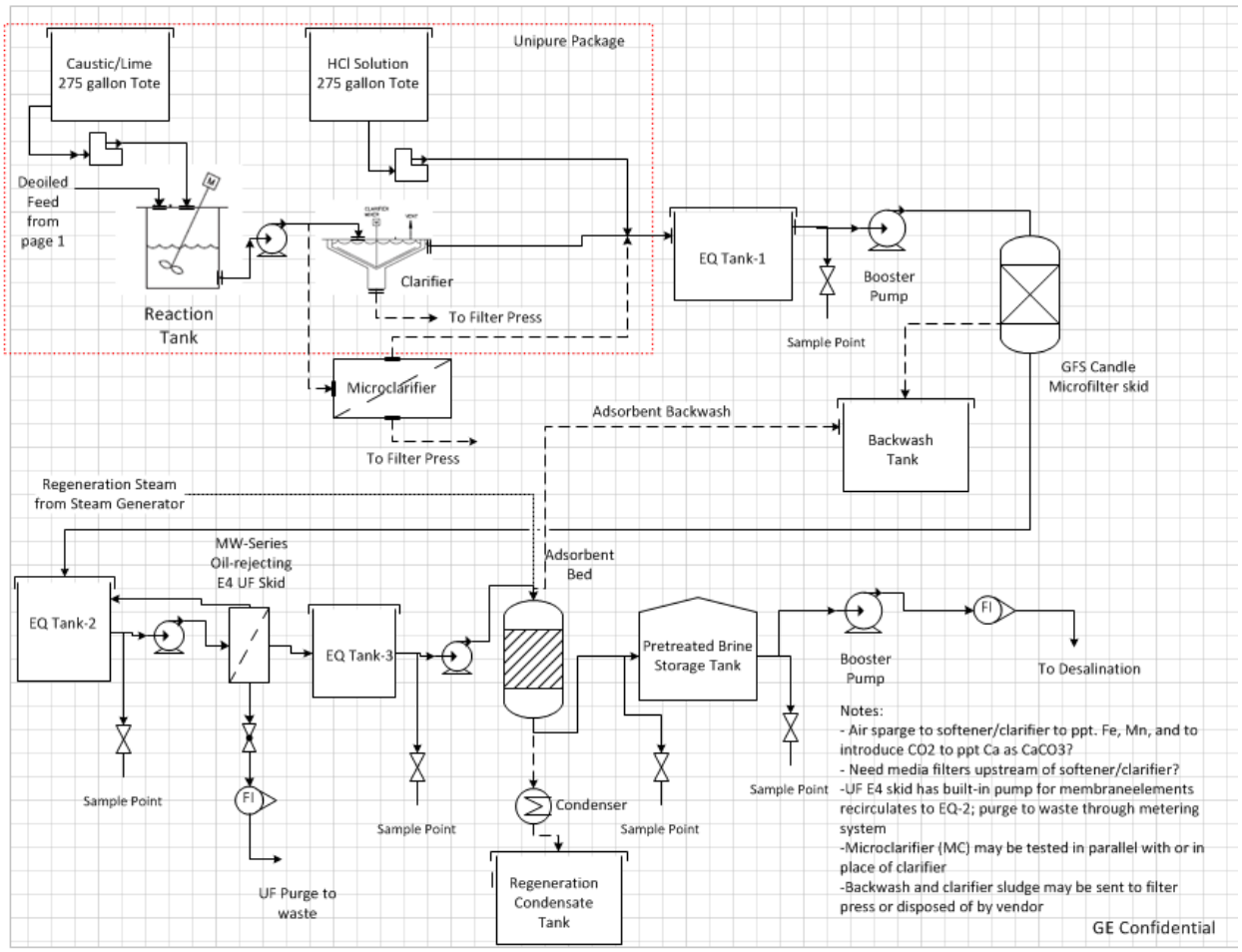

Figure 38. Conceptual Design for Pretreatment

D. Future Efforts

Future efforts should focus on HPRO experimental evaluation, namely the pilot membrane coating experiments described above. Better understanding of the risks associated with HPRO technology, including environmental, regulatory, pretreatment and technical risks, as well as mitigation strategies, will also aid in the understanding, practicality and implementation of HPRO as a cost-effective, high-performance desalination alternative.

Plans should also be made to conduct pilot scale casting experiments, with the goal of fabricating ultrafiltration membrane supports with increased compaction resistance. The pilot coaters, like the ones shown in Figure 39, could be utilized. A phase inversion line could be used to cast the porous ultrafiltration layer, then an interfacial polymerization line could be used to coat the ultrafiltration layer with the thin film polyamide, making the composite RO membrane.

(a)

(b)

Figure 39. GRC Pilot Coating Infrastructure: (a) Phase Inversion Ultrafiltration and (b) Thin Film Interfacial Polymerization Coating Lines.

III. Limitations on Public Release

There are no limitations on public release.

IV. Acknowledgement and Disclaimer

Acknowledgment: "This material is based upon work supported by the Department of Energy under Award Number DE-FE0026308."

Disclaimer: "This report was prepared as an account of work sponsored by an agency of the United States Government. Neither the United States Government nor any agency thereof, nor any of their employees, makes any warranty, express or implied, or assumes any legal liability or responsibility for the accuracy, completeness, or usefulness of any information, apparatus, product, or process disclosed, or represents that its use would not infringe privately owned rights. Reference herein to any specific commercial product, process, or service by trade name, trademark, manufacturer, or otherwise does not necessarily constitute or imply its endorsement, recommendation, or favoring by the United States Government or any agency thereof. The views and opinions of authors expressed herein do not necessarily state or reflect those of the United States Government or any agency thereof."

V. Appendix: Survey of Deep Saline Formation Mineralogy and Water Chemistry

A. Survey of DOE 1260 Sites

Table 29 and Table 30 summarize the five 1260 Phase 1 awardee sites. The rock type and reservoir depth shown in Table 30 can be correlated with formation water composition. For example, Mt. Simon, Lower Tuscaloosa, and Weber are all primarily characterized as sandstone. However, these sandstones vary in their composition and exhibit different geochemical properties and behaviors at different regions and locations. Table 31 shows that the sandstone from the Mt. Simon Formation has a lower percentage of quartz (47.5%) and higher percentages of dolomite (24%) and feldspar (27.9%), compared to the sandstones of the Lower Tuscaloosa and Weber Formations. The Madison Limestone is dominated by dolomite (83%) and calcite (10%). The carbonate reservoir at the Mission Canyon Formation is composed of dolomite (52%), calcite (30%), anhydrite (8.5%), quartz (5%), and illite (3%). Sandstones at the Lower Tuscaloosa Formation have the highest percentage of quartz (79.4%) and chlorite (11.8%).

Table 29. DOE 1260 Phase 1 Site Summary

Prime Contractor; Industrial Partner	Region	Deep Saline Formation	Estimated CO_2 Storage Capacity, Billion tonnes
University of Illinois; Archer Daniels Midland (ADM)	MGSC	Mt. Simon	
Electric Power Research Institute (EPRI); Southern Company	SECARB	Lower Tuscaloosa	
University of Texas at Austin Bureau of Economic Geology (BEG)	SECARB	Lower Trinity Group	
University of Wyoming Carbon Management Institute (CMI)	SWP	Madsion and Weber	
University of North Dakota Energy & Environmental Research Center (EERC)	PCOR	Mission Canyon	65-210

Table 30. Geological Characterization of DOE 1260 Phase 1 Sites

Site	Formation	Injection depth (ft)	Thickness (ft)	Rock type	Porosity (avg, ϕ)	Perm. (avg, md)	Confining unit
UI	Mt. Simon	7,000 [1]	1,506 [1]	Sandstone	0.12 [2]	100 [2]	Primary seal: Eau Clair Fm. (300 -1,000 ft), low-permeability shale and tight limestone. Secondary seal: Ordovician Maquoketa Shale. Tertiary seal: New Albany Shale
EPRI	Lower Tuscaloosa	9,500 [3]	600	Sandstone	0.25 [4]	50-1,000 [4]	Primary seal: Marine Tuscaloosa Fm. (490 ft, ϕ=0.04, k=10^{-4} md); Secondary seal: Austin Fm.; Tertiary seal: Selma Taylor & Navarro Fm.
BEG	Lower Trinity						
CMI	Madison, Weber	11,000	400 [5] 750 [5]	Madison limestone; Weber sandstone	0.10 [5]	10-75 [5]	Chugwater Formation and multiple thick sealing lithologies.
EERC	Mission Canyon	8,050 [6]	700 [6]	Carbonate reservoirs	0.15 [6]	0.35 [6]	Major seals: three aquitard systems. The tight carbonates, anhydrites, and salts serve as a stacked series of seals.

[1] (MGSC, n.d.)

[2] (M. Grobe, 2010)

[3] (Secarb, n.d.)

[4] (Secarb Development , n.d.)

[5] (Surdam, 2011)

[6] (PCOR, n.d.)

Table 31. Mineral Compositions (wt%)

Site	Formation	Rock type	Quartz	Dolomite	Feldspar	Calcite	Chlorite	Illite	Kaolinite	Anhydrite
UI[1]	Mt. Simon	Sandstone	47.5	24.0	27.9	-	-	-	-	-
EPRI[2]	Lower Tuscaloosa	Sandstone	79.4	1.5	0.20	1.5	11.8	1.3	3.1	-
BEG	Lower Trinity									-
CMI	Madison[3]	Limestone	-	83	-	10	-	-	-	6
	Weber[4]	Sandstone	75-95	0-15	5-20	0-15	0-5	0-5	75-95	0-15
EERC[5]	Mission Canyon	Carbonate reservoirs	5.0	52.0	-	30.0	-	3.0	-	8.5

[1] (BEG, n.d.)

[2] (Lu, 2012)

[3] (Chopping, 2012)

[4] (Bowker, 1991)

[6] (Holubnyak, 2011)

B. Formation water chemistry

Formation water is a complex mixture of organic and inorganic compounds. Formation water is typically classified based on its inorganic composition, such as dominant chemical species (e.g. Na, Ca, Mg, Cl) or its salinity (TDS), as shown in Table 32. The formation water chemistry including pH, salinity, salt composition, naturally occurring radioactive materials (NORM), and organics content is critical for evaluating the technical and economic feasibility of formation water treatment and recovery.

Table 32. Formation Water Characterization

Formation water	TDS (mg/L)
Fresh water	0 - 1,000
Brackish water	1,000 - 10,000
Salty water	10,000 - 100,000
Brine water	> 100,000

Formation water chemistry at different sites are summarized in Table 33. The carbonate reservoir at the Mission Canyon formation exhibited the highest concentration of Ca, Mg, and TDS among the five selected sites. This is because the carbonate at the Mission Canyon Formation is primarily composed of dolomite (52%) and calcite (30%), which are reactive and release Ca and Mg from the mineral phase through a dissolution process. This carbonate reservior has reported TOC ranging from 1-18 % and tends to have high organic content compared to other sandstone sites.

The Weber sandstone and Madison limestone formations (located in the same Rock Spring Uplift region) provided a good opportunity to examine the role of mineral composition in determing the formation water chemistry. Higher concentrations of Ca and Mg were found in the Madison Limestone Formation than in the Weber Sandstone Formation due to its higher percentages of dolomite and calcite. The potassium (K) concentration in the Madison Limestone Formation was also higher than in the Weber Sandstone Formation, probably due to higher percentage of feldspar. The potassium-feldspar, which refers to a number of minerals within the feldspar group contains K, thus possibly contributingto the higher K concentration in the Madison formation water.

Table 33. Formation Water Chemistry (units: mg/L)

Site	TDS	Na	K	Ca	Mg	Cl	Br	Sr	TOC
[1] UI	---	51,100	2,060	---	---	120,000	707	---	< 200 [2]
[3] EPRI	138,927	40,733	800	10,108	1,081	---	---	524	200 -1,200 [4]
[5] BEG									
[6] Weber	119,115	43,250	1,940	705	40	61,830	94	---	2,420 [6]
Madison	95,126	32,820	4,210	1,280	170	52,290	115	---	1,940 [6]
[7] EERC	275,089	---	---	19,500	1,338	---	---	---	> 500 [8]

[1] (Panno, 2013)
[2] (Cole, 1987)
[3] (Advanced Resources International, 2009)
[4] (Berch, 2014)
[5] (Lu, 2012)
[6] (Scott A. Quillinan, 2014)
[7] (PCOR, n.d.)
[8] (Jarvie, 2001)

To examine the link between mineralogy and formation water chemistry, the NatCarb brine database was used to generate box-and-whisker plots of formation water chemistry at different locations (NATCARB, 2016), which are shown in Figure 40. There are only four subplots in because the second Weber Formation is currently not available in the database. One advantage of the NatCarb database is that it has multiple measurements spatially distributed across the entire geological formation and thus the data can be statistically analyzed. Figure 40 shows that Na concentrations are the highest among all four formations. Even the "sandstones" have a wide range of cation concentrations. This suggests that specific mineral compositions play an important role in determining formation water chemistry. Although the Lower Tuscaloosa sandstone is not rich in Ca-bearing minerals, it has the highest Ca concentration of the formation waters. This may be attributed to the complex spatial heterogeneity and poor sample representation, given limited core samples for mineral analysis. Rock formations have significant impacts on their water chemistry, however, at this stage, there are no obvious pattern between mineral composition and formation water cation concentrations in Figure 40.

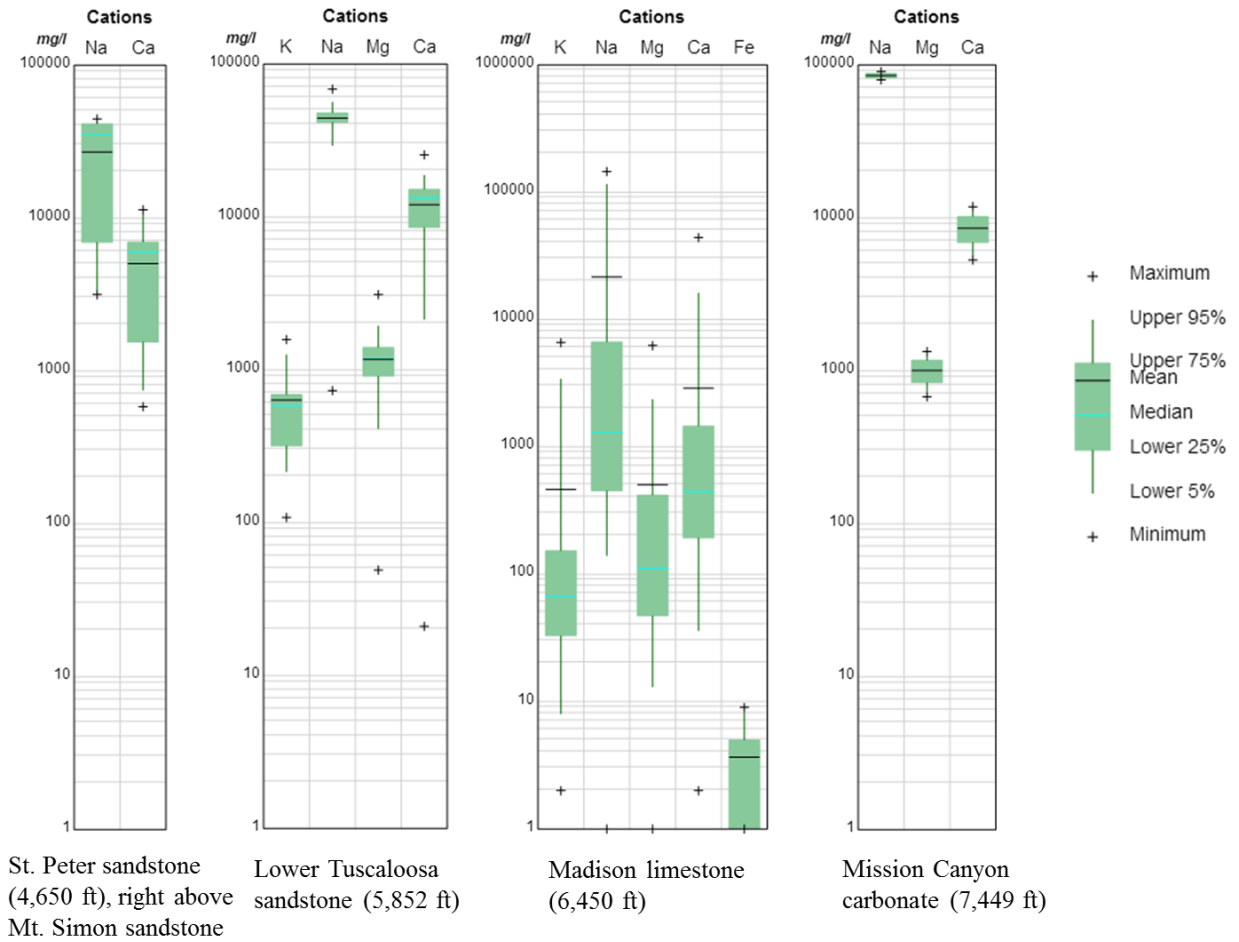

Figure 40. Formation water composition from NatCarb brine database

C. Map of Formation Water TDS and Lithology

Figure 41 shows the spatial pattern of produced water TDS across the U.S. Three red-dotted boxes highlight the higher TDS regions while the yellow box highlights the lower TDS region (Mark A. Engle, 2015). Figure 42 shows lithology information for the United States (USGS, n.d.). The lower TDS region (yellow box) is mainly composited of basalt, a common volcanic rock. The red box that lies within North Dakota is mainly characterized by silt, sand, clay, and sandstone. The red box that includes the Pennsylvania, West Virginia, Ohio, and Michigan state is mainly characterized by shale and sandstone. The red box that includes Texas, Oklahoma, and Kansas is mainly characterized by sand, clay, and silt. Thus, geological

formations with abundant sand, silt, clay, sandstone, and shale typically have high TDS formation waters.

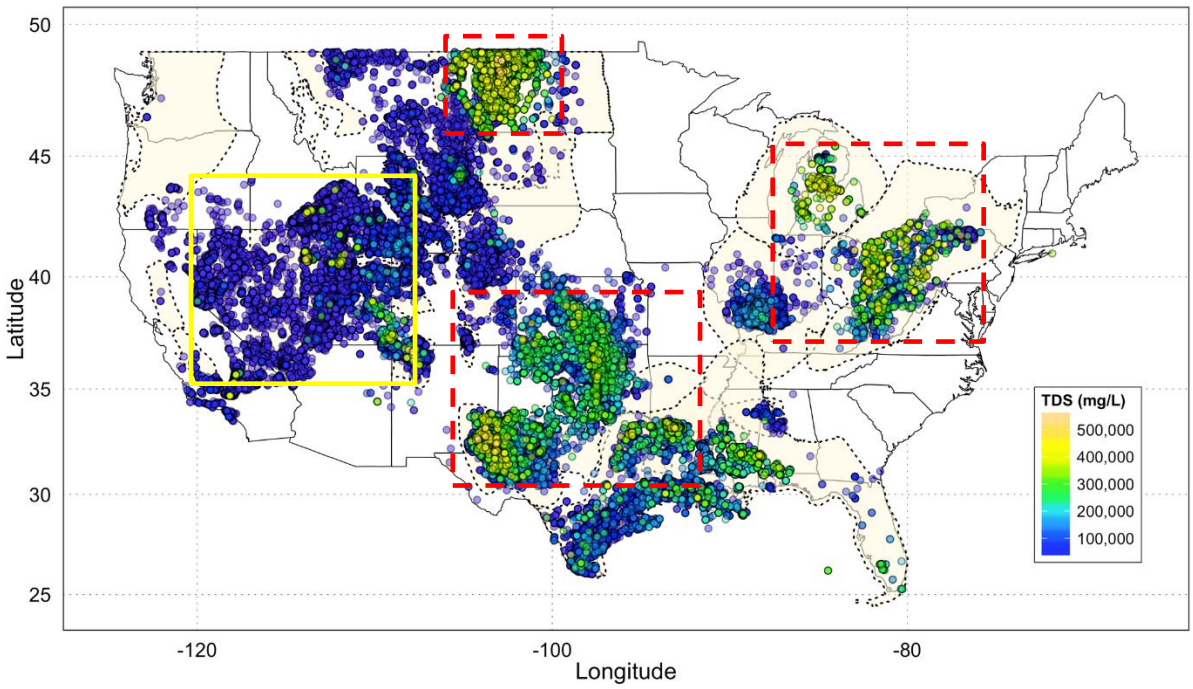

Figure 41. Map of Produced Water TDS

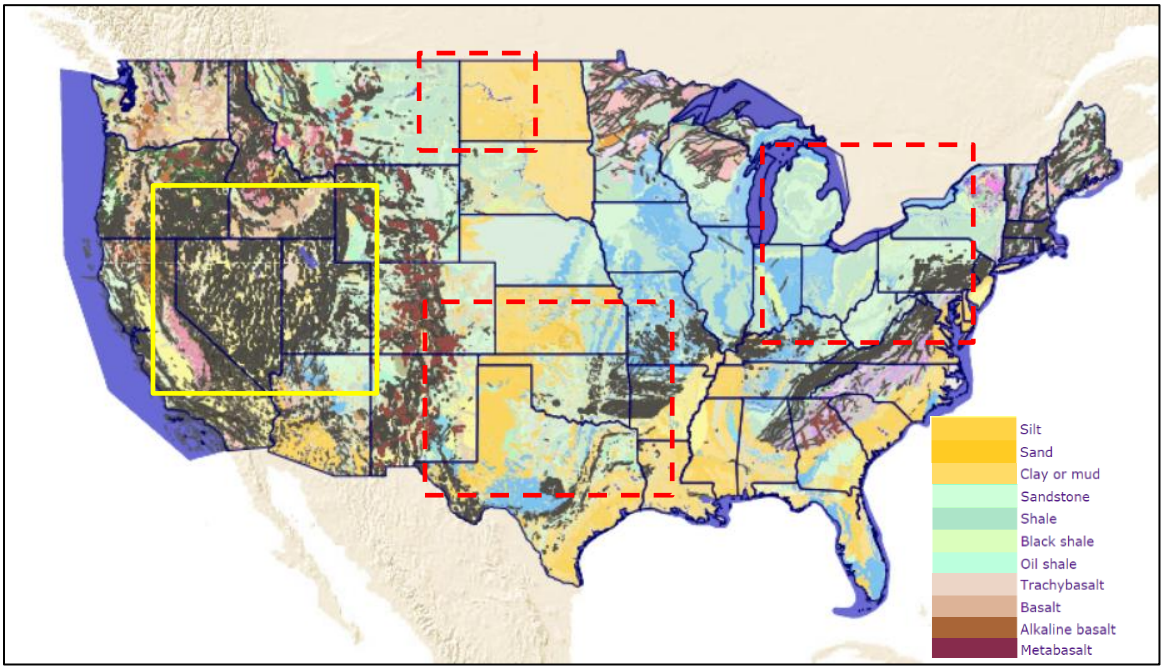

Figure 42. Map of Lithology

VI. Bibliography

(2016). Retrieved from U.S. Geological Survey National Produced Waters Geochemical Database: http://eerscmap.usgs.gov/pwapp/

(2016). Retrieved from U.S. Energy Information Administration: http://www.eia.gov/

(2016, Winter). Retrieved from Rolled Alloys Relative Pricing: www.rolledalloys.com

(2016). Retrieved from Chemical Engineering Plant Cost Index: http://www.chemengonline.com/pci/

(2017). Retrieved from Spiral-wound reverse osmosis element configuration: http://www.lixus.net.cn/en/products/Membrane.aspx

Advanced Resources International. (2009). *Geologic Storage Capacity for CO2 of the Lower Tuscaloosa Group and Woodbine Formation. SECARB Phase III Work Product 1.1.c., Final Report.*

Al-Karaghouli, A., & Kazmerski, L. L. (2013). *Renewable and Sustainable Energy Reviews, 24*, 343.

American Society of Mechanical Engineers (ASME), International Boiler and Pressure Vessel Code (BPVC), Section VII; http://www.engineeringtoolbox.com/asme-boiler-vessel-code-d_8.html. (May 24, 2017).

Baker, R. (2008). *Membrane Technology and Applications; 2nd ed.* West Sussex: Wiley.

BEG. (n.d.). *Brine Formation Database*. Retrieved from http://www.beg.utexas.edu/gccc/CO2_data/aaDataMain.php

Berch, H. a. (2014). *Predicting Potential Unconventional Production in the Tuscaloosa Marine Shale Play Using Thermal Modeling and Log Overlay Analysis.*

Blondes, M., Gans, K., Rowan, E., Thordsen, J., Reidy, M., Engle, M., . . . Thomas, B. (2016). *U.S. Geological Survey National Produced Waters Geochemical Database v2.2 (PROVISIONAL) Documentation.*

Bowker, K. a. (1991). Carbon dioxide injection and resultant alteration of the Weber Sandstone, Rangely Field, Colorado. *AAPG Bulletin*, 1489-1499.

Bradshaw, R., Greathouse, J. C., Simmons, B., & Dedrick, D. a. (2008). *Desalination Utilizing Clathrate Hydrates (LDRD Final Report), SAND2007-6565.* Sandia National Laboratory.

Brooks Rand Labs. (2016). *Specialized Analyses of Flue Gas Desulfurization Wastewater for Heavy Metals.*

Chopping, C. a. (2012). Supercritical carbon dioxide–brine–rock reactions in the Madison Limestone of Southwest Wyoming: An experimental investigation of a sulfur-rich natural carbon dioxide reservoir. *Chemical Geology*, 322–323, 223-236.

Cole, G. D. (1987). Organic geochemistry and oil-source correlations, Paleozoic of Ohio. *AAPG Bulletin* , 788-809.

Dickson, A. G., & Goyet, C. (1994). *Handbook of methods for the analysis of the various parameters of the carbon dioxide system in sea water.*

Freyman, M. (February 2014). *Hydraulic Fracturing & Water Stress: Water Demand by the Numbers.*

GE Power, Water & Process Technologies. (2016). *Flue Gas Desulfurization Wastewater Treatment Solutions.*

Global Water Market. (2017). *Companies and Markets, Volume 1.*

Harto, C., & Veil, J. (2011). *Management of water extracted from carbon sequestration projects.* Argonne National Laboratory (ANL).

Hayes, T. (2011). Characterization of Marcellus and Barnett Shale Flowback Waters and Technology Development for Water Reuse. *Hydraulic Fracturing Technical Workshop #4.*

Heins, W. (2006). *Use of Evaporation for Heavy Oil Produced Water Treatment.* General Electric Co.

Higgins, T. E., Sandy, A. T., & Givens, S. W. (2009). Flue gas desulfurization wastewater treatment primer. *Power (New York)*, 153.

Holubnyak, Y. M. (2011). Investigation of geochemical interactions of carbon dioxide and carbonate formation in the Northwest McGregor oil field after enhanced oil recovery and CO2 storage. *Energy Procedia*, 3612-3619.

International Desalination Association. (2006). *19th IDA Worldwide Desalting Plant Inventory.* Oxford, UK: Media Analytics Ltd.

Jarvie, D. (2001). Williston Basin petroleum systems: inferences from oil geochemistry and geology. *Mountain Geologist*, 19-42.

Kondash, A., & Vengosh, A. (2015). Water Footprint of Hydraulic Fracturing. *Environmental Science & Technology Letters, 2*, 276-280.

Lu, J. K. (2012). CO2–rock–brine interactions in Lower Tuscaloosa Formation at Cranfield.

M. Grobe, J. C. (2010). *Carbon Dioxide Sequestration in Geological Media State of the Science (Aapg Studies in Geology).*

Mark A. Engle, K. D. (2015). Applications of the U.S. Geological Survey Produced Waters Geochemical Database for Environmental Oil and Gas Operations. *International Petroleum Environmental Conference.* Tulsa, OK.

McCutcheon, J. M. (2005). A novel ammonia-carbon dioxide forward (direct) osmosis desalination process. *Desalination*, 1-11.

McGinnis, R. H.-S. (2013). Pilot demonstration of the NH3/CO2 forward osmosis desalination process on high salinity brines. *Desalination*, 67-74.

McGovern, R. K., & Lienhard, J. H. (2014). On the potential of forward osmosis to energetically outperform reverse osmosis desalination. *Journal of Membrane Science*, 245-250.

MGSC. (n.d.). Retrieved from http://www.sequestration.org/mgscprojects/deepsalinestorage.html

Mickley, M. (2008). *Survey of High-Recovery and Zero Liquid Discharge Technologies for Water Utilities.* Alexandria, VA: Water Reuse Foundation.

Narayan, G. P. (2011). Status of humidification dehumidification desalination technology. *IDA World Congress/Perth Convention and Exhibition Centre (PCEC), Perth, Western Australia September 4-9, 2011.*

NATCARB. (2016). Retrieved from http://www.natcarbviewer.com/

Panno, S. H. (2013). Formation waters from Cambrian-age strata, Illinois Basin, USA: Constraints on their origin and evolution. *Geochimica et Cosmochimica Acta*, 181-184.

PCOR. (n.d.). Retrieved from https://www.undeerc.org/pcor/newsandpubs/pdf/RTIP-CO2-Huff-n-Puff-Validation-Test.pdf

Schlag, S., Glauser, J., & Yokose, K. (2008). *CEH Product Review: Sodium Chloride.* SRI Consulting.

Scott A. Quillinan, J. F. (2014). *The Geochemical Characterization of Reservoir Fluids: Defining the Fluid and Rock System and Identifying Changes to Baseline Conditions Due to Well Completion.* Carbon Management Institute.

Secarb Development . (n.d.). *Southeast Regional Carbon Sequestration Partnership - Development Phase*. Retrieved from https://www.netl.doe.gov/publications/factsheets/project/NT42590.pdf

Secarb. (n.d.). *Saline Reservoir Field Test: Mississippi Test Site Fact Sheet*. Retrieved from http://www.secarbon.org/files/mississippi-test-site.pdf

Silva, J., Gettings, R., Kostedt, W., Watkins, V., Hardy, A., & Shapiro, A. (2014). *NORM Mitigation and Clean Water Recovery from Marcellus Produced Water.* Research Partnership to Secure Energy for America (RPSEA).

Silva, J., Gettings, R., Kostedt, W., Watkins, V., Hardy, A., & Shapiro, A. (2014). *NORM Mitigation and Clean Water Recovery from Marcellus Produced Water. RPSEA Final Report.* Houston, TX: RPSEA.

Surdam, R. J. (2011). The key to commercial-scale geological CO2 sequestration: Displaced fluid management. *Energy Procedia*, 4246-4251.

Technical Bulletin: Water Quality Variability During Oilfield Wastewater Treatment for Frac Reuse. (2016). Retrieved from Rock Water Energy Solutions: http://www.rockwaterenergy.com/case-studies/water-quality-variability-during-oilfield-wastewater-treatment-for-frac-reuse/

Ulrich, G., & Vasudevan, P. (2004). *Chemical Engineering Process Design & Economics: A Practical Guide, Second Edition.*

USGS. (n.d.). *USGS Database*. Retrieved from http://mrdata.usgs.gov/geology/state/map.html#

Whitman, C., Mysyk, R., & White, M. (2008). Investigation of factors affecting crystallization of cyclopentane clathrate hydrate. *The Journal of Chemical Physics*, 1-6.

Yarlagadda, S., Camacho, L., Gude, V., & Wei, Z. a. (2009). Membrane distillation for desalination and other separations. *Recent Patents on Chemical Engineering*, 128-158.

Zander, A., Elimelech, M., Furukawa, D., Gleick, P., Herd, K., Jones, K., . . . Vaux, H. (2008). *Desalination: A national perspective. National Research Council, The National Academies.*